DESIGNED ADAPTED TOOLS FOR ENERGY MANAGEMENT WITH ENERGY STORAGES IN HUC

D.T3.1.2

Project summary:

It is challenging to provide a low carbon energy supply in cities with energy storages. Especially in historical urban centres it is very difficult to achieve these results, because interventions in this specific area meet strict architectural protection constraints, involve higher implementation costs and often come in conflict with town planning policies.

Therefore, the main objective is to improve and enrich energy and spatial planning strategies targeting historical city centres by focusing on integration of energy storage systems to enhance the public institutional and utility capabilities.

The pilot actions implemented in specific sites will demonstrate the various energy storages that can be adapted and transferred to other local or regional environments. The storages will provide good show-cases to the local authorities which can benefit in sense of improved energy efficiency, increased usage of renewable energy sources and lower costs for energy. The transnational strategy will provide the recommendations for improving the energy and spatial planning. The energy management tool will enable to monitor all features that prove the effectiveness of the pilot installations. Additionally, the autarky rate tool will indicate the economic and reasonable utilisation of storages. By establishing the stakeholder deployment desk Store4HUC will reach the relevant players to share the knowledge and also transfer it to other additional audience. It will enable to gain wider consensus of the pilot instalment and further tool usage, especially with the signed memorandums of the future tool utilisation. The project approach foresees also peer review actions, mutual learning within project consortium and exchange of experiences and knowledge with target groups that can enhance the transnational added value. Innovative energy storage installation and storing of renewable energy determines the innovative aspect of Store4HUC.

WPT3 description:

In WPT3 the objective is to present the impact of integration of energy storage systems in HUC. Based on the technical & legal framework of integrating efficiently energy storage systems in HUC affordable solutions will be used to demonstrate the matured combination of renewable energy sources & energy storages. Both will be controlled via adapted EMS tool able to maintain & to balance the overall system. Available experiences of selected case study sites and of other running projects will be used in a consolidated way. This foremost relates to energy management software tools inherited by partners from preview projects like e.g. Interreg Danube 3Smart which is coordinated by this WP leader – PP9. The tools adaptation will be concepted, realized and finalized through pilot verifications and interactions, by development PPs (PP9, PP4). After that the establishment of a software tool to interpret autarky rates due to the integration of RES in HUC occurs. The autarky rate is interpreted with an additional checklist. Economical, technical and ecological impacts of the calculated autarky rate are evaluated. Furthermore, it will be examined which performance effects are generated from different renewable energy sources. The gathered information will then be presented via the online tool which will be available for the public for free. An online guide will be elaborated guiding the users through the relevant functions of the tool. Every partner will be trained in the use & all partners will afterwards organize training sessions with members of the deployment desks & invited external experts to educate them on the use & to show corresponding benefits. The acceptance and further usage of the tool will be agreed within the deployment desks and officially committed with the signed memorandum of understanding for the future use of the tools. It is anticipated to engage 8 additional institutions (public institutions, public utilities, etc.) applying for the tools via deployment desks.

Title:	Designed adapted tools for energy management with energy storages in HUC
Deliverable:	D.T.3.1.2
Authors:	Mario Vašak, Filip Rukavina, Vinko Lešić, Mateja Car, Alois Kraussler, Robert Pratter
Contributors:	Reiterer & Scherling GmbH
Status:	Final
Reviewed by:	Katja Karba, Michael Heidenreich
Submission:	13 June 2020

Notations and acronyms

EMS	Energy Management System
Autarky rate	Assessment of installation self-sufficiency
PV	Photo-voltaic
DSO	Distribution System Operator
CHP	Combined Heat and Power
LP	Linear Program
SLP	Sequential Linear Program
HUC	Historical Urban Centre

Table of contents

Executive summary

Energy management systems optimally reconcile conflicting requirements for utility and energy performance of systems. This is even harder and even more needed for different systems placed in historical urban centres where additional constraints are stemming from cultural heritage preservation regulations.

This is a design document for the software modules of the tool for energy management in historical urban centres, tailored for application on pilot sites of the Store4HUC project.

It relies on the previously developed concept of the energy management tool where several software modules are inherited from the preceding Interreg Danube project 3Smart and in general the tool is based on ideas from 3Smart. The design of new modules used on the pilot sites of the Store4HUC project is presented in this deliverable – foremost these are (i) module for optimal parametrization of the PV and battery storage system and (ii) module for optimal operation of the heat sources connected to a heat storage.

1. Introduction and general considerations on energy management systems

Energy management systems (EMSs) have in general the task to consolidate the operation of complex systems constituted of different energy-relevant parts, such that they optimally interact with each other from the point of view of energy they use.

The optimality of this interaction is set via goals for operation of the considered complex system expressed as objective function and via constraints on different physical quantities in that system that need to be obeyed.

The objective function and the mathematical constraints formulation constitute the mathematical optimization problem which is posed by specific software modules based on provided input data for the system in question. The software tools developed have the main purpose to efficiently construct the optimization problem from input data, call the appropriate solver to solve the optimization problem efficiently and process its output results to finally provide the advice for system parametrization or operation (off-line) or a direct command for operation to the automation system (on-line).

The concept of energy management tool for the historical urban site is developed within the previous deliverable D.T3.1.1 [1]. The tool developed for energy management of historical urban centres (HUCs) is tailored from the developed energy management tool of the Interreg Danube project 3Smart [2].

There are two new modules that were not a part of 3Smart and that have arisen as a need for optimal parametrization, planning and operation of energy storages at HUCs, and the focus of this deliverable is put on them. They are [1]:

(1) module for optimal sizing of the investment in a renewable electricity source and electricity storage for a particular consumer with known electricity consumption profile under given condition of allowed return on investment period and HUC-specific constraints, with included profiling of optimal operation of the storage system;

(2) module for optimal operation of the combination of heat sources and a heat storage system for a particular consumer or producer with known heat demand and required temperature conditions in the heating medium storage (on-line operation of this module is module (12) from the concept).

Compared to the concept, for the case of module (2) parameterization of the heat storage is opted out due to revealed significant computational complexity behind that would prevent its usage in practice.

In the sequel of this deliverable first in Section 2 the design of modules (1) and (2) is presented, and then in Section 3 their application to the Store4HUC pilot sites is illustrated. Module (1) is applied to the pilot sites Bračak and Cuneo, while module (2) is applied to the pilot sites of Bračak, Lendava and Weiz.

2. Design of the energy management tool adapted to historical urban centres

2.1. Module (1)

Module (1) of the energy management tool for historical urban centres is used for optimal sizing of the investment in a renewable electricity source and electricity storage for a particular consumer with known electricity consumption profile under given conditions of allowed return on investment period and HUC-specific constraints and with included profiling of optimal operation of the battery storage system.

Inputs of the module are: historical electricity demand, renewable electricity source and storage unit price per power and energy capacity, given return on investment period, grid pricing conditions, HUC-induced constraints

Outputs of the module are: renewable energy source and storage optimal power and energy size, optimal profile of battery storage operation throughout the observation period (preferably one full year).

The currently designed procedure is tailored for the combination of the photovoltaic system and battery storage system. Optimal size of the PV system in terms of its power production at STC (standard test conditions: 1000 W/m2 input irradiance and 25°C PV modules temperature) is provided, as well as the optimal size of the battery storage system in terms of its power converter power rating and the storage capacity. The mentioned optimal parameters are computed based on the measured electrical energy consumption at the consumer's grid connection point, and a PV energy production. As the PV system is yet to be installed, PV measurements of a nearby site with the peak power of $P_{PV,peak,nearby}$ can be used. The length of the measurement window is recommended to be 1 year long to capture all seasons. Resolution of those measurements (denoted with T_s in the sequel) must be the same as the resolution used by the DSO of the utility grid in order to accurately calculate the peak power billing.

At every time instance k before any PV or battery system installation, energy consumed (demand) is equal to the energy coming from the grid: $E_{demand}(k) = E_{grid}(k)$. By adding a PV and a battery system, energy conservation equation that defines overall energy exchange between the HUC and the grid becomes:

$$E_{demand}(k) = E_{grid}(k) - E_{ch}(k) + E_{dch}(k) + \alpha_{PV} E_{PV}(k), \qquad (2.1.1)$$

where E_{ch} and E_{dch} are energies of charging and discharging the battery, with power converter efficiencies already included. E_{PV} is the energy from a PV system, measured at a nearby location, and α_{PV} is the scaling coefficient used to calculate the optimal peak power of the new PV system with respect to the existing one: $\alpha_{PV} = \frac{P_{PV,peak}}{P_{PV,peak,nearby}}$.

Optimal parametrization of a PV and battery system add-on can be formulated as a linear programming problem:

$$Minimize\ f^T x,$$
$$subject\ to\ A_{ineq} x \leq b_{ineq},$$
$$A_{eq} x = b_{eq}, \qquad (2.1.2)$$
$$x_{min} \leq x \leq x_{max},$$

where x is a vector of optimization variables and $f^T x$ is a linear cost function that needs to be minimized. A_{ineq} and b_{ineq} are matrix and vector of inequality constraints, and A_{eq} and b_{eq} are matrix and vector of equality constraints. x_{min} and x_{max} are lower and upper bounds of x. Vector x contains, inter alia, the following elements:

- $E_{ch}(k)$, energy charging the battery at every time instance k (from kT_s to $(k + 1)T_s$) in kWh,

- $E_{dch}(k)$, energy discharging the battery at every time instance k in kWh,

- $E_{g,pos}(k)$, energy taken from the grid at every time instance k, $E_{g,pos} = \max(0, E_{grid})$, in kWh,

- $P_{g,max}(l)$, incurred peak power in the billing interval l, in kW,

- SoC_0, state of charge of the battery system at time instance 0 in kWh,

- $E_{bat,max}$, capacity of the battery system in kWh

- $P_{PC,max}$, power rating of the power converter of the battery system in kW

- α_{PV}, scaling coefficient for the peak power of the PV system

- additional auxiliary variables for calculation of peak power if the billing formula is non-linear (but convex). For example, $P_{g,n}$, contracted peak power in kW.

To make sure the calculated sequence is repeatable, the last instance of state of charge must be equal to the starting one: $SoC(0) = SoC(N)$. From this expression comes the first (and only) equality constraint:

$$\sum_{k=0}^{N-1} \eta_{ch}\, E_{ch}(k) - \sum_{k=0}^{N-1} \eta_{dch}\, E_{dch}(k) = 0, \qquad (2.1.3)$$

where η_{ch} and η_{dch} are charging and discharging efficiencies of the battery system

Charging and discharging the battery at the same time should not be allowed, but this constraint cannot be written in a linear form. Therefore, a constraint from [3] is used:

$$E_{ch}(k) + E_{dch}(k) \le P_{PC,max} Ts. \qquad (2.1.4)$$

Because of the power converter efficiencies, the linear program will never choose a scenario with simultaneous charging and discharging as long as it is beneficial to always spend less energy (i.e. if the energy prices for energy exchange with the grid are positive). For some special cases, like instances with negative prices, this constraint ensures that all solutions are physically possible on the battery system.

To make the planned investment in the PV and battery system economically viable, and assuming that the observed period is 1 year, an inequality constraint is introduced:

$$cost\ of\ energy\ without\ investment - cost\ of\ energy\ with\ investment$$
$$\ge \frac{cost\ of\ investment}{number\ of\ years\ to\ payoff} + yearly\ maintenance. \qquad (2.1.5)$$

This way, one can define in which period the investment should pay off. The longer the payoff period is, the higher the investment could be. Yearly maintenance is defined as a sum of degradation costs of each element of the system. For the PV system and the power converter, that is the price of the element divided by the number of years that element can last. Degradation cost of the battery is calculated as:

$$J_{deg,bat} = \frac{c_{bat}}{2 n_{cyc} DoD} \left(\sum_{k=0}^{N-1} E_{ch}(k) + E_{dch}(k) \right), \qquad (2.1.6)$$

where c_{bat} is the price of the batteries in the battery system per unit of energy, n_{cyc} is the number of charge-discharge cycles of the battery during its lifetime, and DoD is the allowed depth of discharge of the battery.

Other inequality constraints are as follows:

- $0 \le E_{ch}(k) \le P_{PC,max} T_s$

- $0 \le E_{dch}(k) \le P_{PC,max} T_s$

- $(1 - DoD) E_{bat,max} \le SoC(k) \le E_{bat,max}$

- $0 \leq \alpha_{PV} \leq \alpha_{PV,max}$

- $0 \leq P_{PC,max}$

- additional constraints for calculation of peak power billing (country- and site-wise specific),

where T_s is the period of measurement samples (resolution), and $\alpha_{PV,max}$ is a value that limits the PV size because of physical restrictions related to the PV installation placement. E.g. for longer payoff periods it would be optimal to install more PVs, but one cannot install more than the physical capacity dictates, which may be also related to adherence to different cultural heritage protection rules.

The cost function for the linear programming problem, that should be minimized, can be defined in multiple ways, depending on the historical site requirement and other factors. Three of them are defined, aligned with KPIs definition from [4]:

1) overall energy taken from the grid (not accounted energy provided to the grid) – KPI$_1$

2) price of the overall energy taken from the grid – KPI$_2$;

3) price of the overall energy taken from the grid + price of the investment yearly scaled with respect to the fixed payoff period + price of the yearly maintenance of the PV and battery system;

Each of them yields a different result, but all of them due to constraint (4) satisfy the condition of investment pay-off after the end of the set pay-off period. Using function 3) yields the most conservative result in terms of the PV, battery, and power converter sizes since the total scaled yearly cost is minimized. Using cost function 1) yields largest sizes of the battery capacity and power converter power. In that case exchange of energy with the grid would be minimized and the so-called self-sufficiency or autarky of the system maximized, so the battery system would be utilized the most. Using function 2) yields results that are inbetween, with tendency to use larger power capacity of the storage to minimize peak power costs.

For the case where the billing formula of the peak power is non-linear (but convex), the programme also calculates the optimal contracted peak power, $P_{g,n}$ for the consumer. Therefore, it is providing optimal energy pricing for the consumer even for the case when add-ons are not economically viable ($\alpha_{PV} = E_{bat,max} = P_{PC,max} = 0$).

2.2. Module (2)

Module (2) of the energy management tool for historical urban centres is the module for optimal operation of the combination of heat sources and a heat storage system, for a particular consumer or set of consumers connected to the storage, with known cumulative heat demand under required heating medium temperature conditions in the storage. The module results in profiling of optimal operation of heat generation systems that inject heat in the storage.

Inputs of the module are historical heat demand, simple efficiency-based heat sources models and operational constraints and/or grid pricing conditions (if heat is supplied from a local heat distribution grid), storage model which usually includes stratification effects, HUC-induced constraints.

Outputs of the module are the optimal profiles of heat sources engagement throughout the observation period.

The procedure of finding the optimal profiles of heat sources engagement is based on the heating demand and disturbances. Since the module works for day-ahead operation, heating demand and disturbances must be predicted. To test functionality of the module in a simulation, one can use pre-recorded heating demand and disturbances. The main disturbance for a heat storage system is the temperature of air around the storage tank due to imperfect insulation. The length of profiles, both inputs and outputs, is 24 h, and the

resolution of measurements is equal to 15 min, which is short enough to capture dynamic behaviour of the system, but also long enough not to make the module computationally too expensive.

2.2.1. Mathematical model

The centre of the mathematical model is the stratified heat storage tank where each layer is modelled separately. Starting from a simple energy balance on an individual layer, the change in the energy of the layer per time is the difference between the sum of the rates of energy entering and the sum of the rates of energy leaving the layer [5]:

$$\frac{dE}{dt} = \sum \dot{E}_{in} - \sum \dot{E}_{out},$$
(2.2.1)

where energy of a single layer l is expressed as

$$E_l = m_l c_p T_l.$$
(2.2.2)

Specific heat capacity of the heating medium c_p changes just slightly with the change of temperature, but here is considered constant for the sake of simplicity, as well as mass of the heating medium, m_l. Therefore, the only variable that changes through time is temperature T_l. Ways of energy coming into the layer are:

- bulk transport into the layer,
- conductive heat transfer from an adjacent node at a higher temperature,
- buoyancy effect from the layer beneath if it is at a higher temperature,

while rates of energy leaving the layer are:

- bulk transport from the layer,
- conductive heat transfer from an adjacent node at a lower temperature,
- buoyancy effect from the layer above if it is at a lower temperature,
- convective heat transfer through the walls of the tank (assuming that the temperature of the layer is greater than the temperature of the ambient air outside the tank).

Figure 1 shows a symbolic representation of a layer in a storage tank with its adjacent layers. q represents mass flow, k_c is coefficient of thermal conductivity, k_b is coefficient of buoyancy effect, and h is convective heat transfer coefficient between heating medium and outside air.
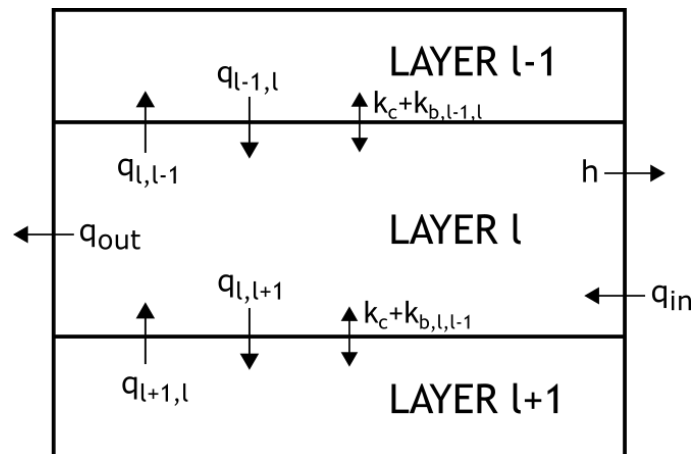
Figure 1. Symbolic representation of a layer in a storage tank.

Following equation (2.2.1) and Figure 1, the ordinary differential equation for the layer l becomes:

$$m_l c_p \frac{dT_l}{dt} = q_{l-1,l} c_p T_{l-1} + q_{l+1,l} c_p T_{l+1} + q_{in} c_p T_{in} - q_{l,l-1} c_p T_l - q_{l,l+1} c_p T_l - q_{out} c_p T_l$$

$$+ \left(k_c + k_{b,l-1,l}\right) \frac{A_h}{\Delta x_{l-1,l}} (T_{l-1} - T_l) - \left(k_c + k_{b,l,l+1}\right) \frac{A_h}{\Delta x_{l,l+1}} (T_l - T_{l+1}) \quad (2.2.3)$$

$$- h A_{w,l}(T_l - T_{env}).$$

Heating medium can flow through a storage tank only in one direction so flows between layers take on non-negative values, i.e. if $q_{x,y} > 0$ then $q_{y,x} = 0$. Mass flow q_{in} can be return line from a heating circuit or a heating source, while q_{out} can be supply line for a heating circuit or a heating source.

A_h is area bordering adjacent layers, which is the same for all layers in a cylindrically shaped tank. $\Delta x_{x,y}$ is geometric distance between layers which in this case is equal to the distance between centres of layers x and y.

Coefficients of conductive heat transfer k_c and convective heat transfer coefficient h are taken from engineering tables and they are considered constant for the same reason as specific heat capacity c_p. Buoyancy effect here is seen as buoyant conductivity and its coefficient is given as in [6]:

$$k_{b,l-1,l} = \begin{cases} \kappa^2 d^2 \sqrt{g \alpha_p \frac{T_l - T_{l-1}}{\Delta x_{l-1,l}}}, when \ T_l > T_{l-1} \\ 0, otherwise, \end{cases} \quad (2.2.4)$$

where κ is Von Karman constant (≈ 0.4), d is the diameter of the tank, g is the acceleration of gravity, and α_p is thermal expansion coefficient of the heating medium at constant pressure taken as a constant.

Temperature of the medium entering the tank T_{in} is modelled through the equation for the power of a device where it comes from, $P_{hs} = q_{hs} c_p \left(T_{hs,out} - T_{hs,in}\right)$ for a heat source (hs), and $P_{hc} = q_{hc} c_p \left(T_{hc,in} - T_{hc,out}\right)$ for a heating circuit (hc). If the medium for a device is supplied from layer k, temperature T_{in} can be replaced with:

$$T_{in} = \begin{cases} T_k + \frac{P_{hs}}{q_{hs} c_p}, if \ heat \ source \\ T_k - \frac{P_{hc}}{q_{hc} c_p}, if \ heating \ circuit. \end{cases} \quad (2.2.5)$$

Every heat source has limits on the temperature it can be supplied with, so it is usually equipped with a bypass valve to ensure safe operation of the heat source when temperature on the inlet is lower than its lower limit. Scheme of such installation is shown in Figure 2.
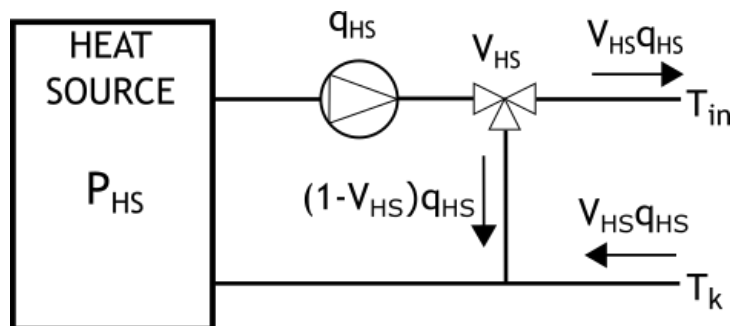
Figure 2. Scheme of a heat source and a bybass valve

Mathematically, bypass valve can take on values in range from 0 to 1 which represent percentages of flow it directs to the direct branch. Therefore, mass flow in the direct branch will be $V_{hs} q_{hs}$, and $(1 - V_{hs}) q_{hs}$ in the bypass branch. If the temperature coming from the tank is greater than minimal temperature required for the operation of the heat source, $T_k \geq T_{hs,in}^*$, bypass valve will direct all the flow through the direct branch: $V_{hs} = 1$. On the other hand, if the temperature coming from the tank is lower than minimal

temperature required for the operation of the heat source, $T_k < T^*_{hs,in}$, bypass valve will be set so that the temperature entering the heat source is equal to the minimal required one: $V_{hs} = \frac{P_{hs}}{P_{hs}+q_{hs}c_p(T^*_{hs,in}-T_k)}$. All together is written as:

$$V_{hs} = \begin{cases} 1, when\ T_k \geq T^*_{hs,in} \\ \frac{P_{hs}}{P_{hs} + q_{hs}c_p(T^*_{hs,in} - T_k)}, when\ T_k < T^*_{hs,in}. \end{cases} \qquad (2.2.6)$$

This behaviour introduces different dynamics to the system depending on the temperature of the layer where heating medium is taken from, T_k. Consequently, for every heat source there will be 2 areas of operation bounded by the minimal input temperature $T^*_{hs,in}$.

Some heat sources also have a maximal input temperature. If the input temperature exceeds that value, the heat source simply shuts down. Some heat sources have a significant decrease in power with rising input temperature which is also modelled. The maximum power profile of a heat source with all the effects considered, is charted in Figure 3.
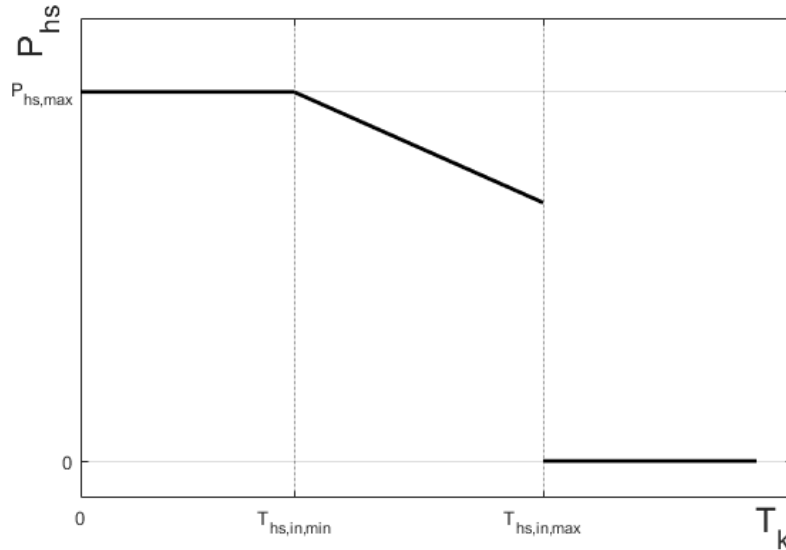
Figure 3. Maximal power profile of a heat source.

All the equations so far are determining non-linear continuous-time models, which need to be linearized and then discretized for the application of this Module. Linearization is performed in a working point to obtain models to fit the notation of a state-space model:

$$\begin{aligned} \dot{x} &= A_{cont}x + B_{cont}u, \\ y &= C_{cont}x + D_{cont}u, \end{aligned} \qquad (2.2.7)$$

where x are the states of the model, u are the inputs to the model, and y are the outputs of the model. In this case states of the model are temperatures of the heating medium in each layer, $T = [T_1 \quad \dots \quad T_n]^T$, where n is the number of layers used in the model of the stratified storage tank. Controllable inputs to the model are powers from heat sources, $u = [P_1 \quad \dots \quad P_m]^T$, where m is the number of heat sources. Uncontrollable inputs are heat demand (P_{dem}), demand flow (q_{dem}) and disturbances ($d_{dist} = [d_{dist,1} \quad \dots \quad d_{dist,nd}]$), so the full vector of uncontrollable inputs is $d = [P_{dem} \quad q_{dem} \quad d_{dist}]^T$. The module for each site must be customized by the developers, since the model largely depends on the architecture of the heat storage system (type of storage system, plumbing, number of sensors on the storage tank, heights at which the medium is taken/returned, …) and way of operation. After linearization, using this module's notation, equation (2.2.7) becomes:

$$\dot{T} = A_{cont}T + B_{u,cont}u + B_{d,cont}d + B_{f,cont}1_{1\times n},$$
$$y = I_n T, \tag{2.2.8}$$

where $B_{f,cont}$ is the constant member as a residual from linearization (for linearization outside stationary points of the system). Additional adjustment is made to fit the model to the original state-space notation by introducing vector of inputs as $v = [u^T \quad d^T \quad 1_{1\times n}]^T$:

$$\dot{T} = A_{cont}T + B_{cont}v,$$
$$y = I_n T, \tag{2.2.9}$$

where $B_{cont} = [B_{u,cont} \quad B_{d,cont} \quad B_{f,cont}]$. Models are then discretized using ZOH (zero-order hold) method to obtain a discrete-time linearized model:

$$T(k+1) = A_{disc}(k)T(k) + B_{disc}(k)v(k). \tag{2.2.10}$$

Matrices A_{disc} and $B_{u,disc}$ are different for every time instant k which represents time interval $[kT_s \quad (k+1)T_s)$. This model can be applied to shifts (denoted with Δ) in temperatures and powers:

$$\Delta T(k+1) = A_{disc}(k)\Delta T(k) + B_{u,disc}(k)\Delta u(k). \tag{2.2.11}$$

Matrices $B_{d,disc}$ and $B_{f,disc}$ are not in this equation since they are multiplying constants.

2.2.2. Algorithm

Since the model is non-linear, linear programming (LP) is not applicable here, but sequential/successive linear programming (SLP) is. The operation of SLP here is to linearize the model in a sequence of points along the prediction horizon, discretize them, apply LP to this sequence of linear models and with it obtain a move towards the optimal solution, but with a constraint within LP not to change the current area of operation. The area of operation change is allowed for the next iteration if the area border is reached with the solution in the current iteration. The iterations are repeated until the solution gets to be stationary or cycling which indicates a local optimum found. The full SLP procedure is as follows:

1. Load predicted (or measured) heat demand and disturbance profiles.

2. Set parameters and initial conditions ($T(0)$ and $u(0)$).

3. Start iterating:

   3.1. Simulate the behaviour of the continuous-time non-linear model of the storage+heat sources system to obtain state values $T(k)$ for each time instance $k = \{1 .. N\}$, where N is the length of prediction horizon in discrete time (N=96 to encompass 24 h of operation).

   3.2. If it is the first iteration, define specific areas of operation for each time interval $k = \{0 .. N-1\}$, along the prediction horizon.

   3.3. Linearize the model on each time interval $k = \{0 .. N-1\}$, to obtain N linearized models for the time intervals along the prediction horizon.

   3.4. Discretize each of the N linearized models.

   3.5. Define the LP problem of slight improvement of the storage+heat sources system operation with N discrete-time linearized models, and such constraints that each model stays in its original specific area of operation.

   3.6. Solve the LP problem.

   3.7. If the edge of a specific area of operation is reached at a certain discrete time-step, if possible, switch the area of operation to the neighbouring one for the next iteration.

4. Iterate until satisfactory level of convergence in the solution of the LP problem is achieved.

The LP itself is defined in expression (2.1.2). Vector x contains, inter alia, the following elements:

- $\Delta T(0)$, change of initial temperatures of each layer of the stratified storage tank,
- $\Delta u(k)$, change of powers of each heat source at every time instance k,
- ε_{T1}, ε_r, auxiliary variables for a routine of introduction of linear norms of optimization variables in the optimization problem.

To avoid having all $\Delta T(k)$ in the optimization vector, an expression to map shift in powers to shift in temperature is used:

$$\Delta T = \alpha\,\Delta T(0) + \beta\,\Delta u, \tag{2.2.12}$$

where $\Delta T = [\Delta T(0)^T \quad \Delta T(1)^T \quad \dots \quad \Delta T(N)^T]^T$, $\Delta u = [\Delta u(0)^T \quad \Delta u(1)^T \quad \dots \quad \Delta u(N-1)^T]^T$, and α and β are matrices derived from the N discretized linear models using equation (2.2.11):

$$
\begin{aligned}
&\Delta T(0) = I_n \Delta T(0)\\
&\Delta T(1) = A_{disc}(0)\Delta T(0) + B_{u,disc}(0)\Delta u(0)\\
&\Delta T(2) = A_{disc}(1)A_{disc}(0)\Delta T(0) + A_{disc}(1)B_{u,disc}(0)\Delta u(0) + B_{u,disc}(1)\Delta u(1)\\
&\dots\\
&\Delta T(k) = \prod_{j=k-1}^{0} A_{disc}(j)\,\Delta T(0) + \sum_{j=0}^{k-1}\left(\prod_{l=k-1}^{j+1} A_{disc}(l)\right) B_{u,disc}(j)\Delta u(j)\\
&\dots
\end{aligned}
\tag{2.2.13}
$$

Finally, matrices α and β are:

$$
\alpha = \begin{bmatrix} \alpha(0)\\ \alpha(1)\\ \vdots\\ \alpha(N)\end{bmatrix}, \text{where } \alpha(k) = \begin{cases} I_n, for\ k = 0\\ \displaystyle\prod_{j=k-1}^{0} A_{disc}(j), for\ k \in [1,N]\end{cases}
\tag{2.2.14}
$$

$$
\beta = \begin{bmatrix}\beta(0)\\ \beta(1)\\ \vdots\\ \beta(N)\end{bmatrix} = \begin{bmatrix}\beta(0,0) & \beta(0,1) & \dots & \beta(0,N-1)\\ \beta(1,0) & \beta(1,1) & \dots & \beta(1,N-1)\\ \vdots & \vdots & \ddots & \vdots\\ \beta(N,0) & \beta(N,1) & \dots & \beta(0,N-1)\end{bmatrix}, where
$$

$$\tag{2.2.15}$$

$$
\beta(k,j) = \begin{cases} 0, for\ k \le j\\ \displaystyle\left(\prod_{l=k-1}^{j+1} A_{disc}(l)\right) B_{u,disc}(j), for\ k > j\end{cases}
$$

To make sure the calculated sequence is repeatable, the last instance of medium temperatures must be equal to the starting one, but such a hard constraint could lead to an infeasible solution. Therefore, this constraint is relaxed by adding auxiliary variables ε_r:

$$\varepsilon_r = \left| T(0) + \Delta T(0) - \big(T(N) + \Delta T(N)\big)\right|, \tag{2.2.16}$$

which are then strongly penalized in the cost function. Absolute value in (2.2.16) is to be interpreted component-wise, and since absolute is not a linear function, the equality is transformed into a group of inequalities, also using equation (2.2.12):

$$
\begin{aligned}
&\varepsilon_r \ge -T(0) + T(N) + (\alpha(N) - I_n)\Delta T(0) + \beta(N)\Delta u,\\
&\varepsilon_r \ge T(0) - T(N) - (\alpha(N) - I_n)\Delta T(0) - \beta(N)\Delta u.
\end{aligned}
\tag{2.2.17}
$$

Another important constraint is the operating interval for the layer of the tank from which the heating medium is supplied. It is usually the top layer, so its temperature is denoted with T_1. Heating circuits need to have medium temperature in certain interval, which for LP would be $T_{1,min} \le T_1(k) + \Delta T_1(k) \le T_{1,max}$. LPs have tendency to give solutions that are on the border of feasible solution, and counting in the error

introduced by linearization, this hard constraint can lead to an infeasible solution. That is the reason for relaxing this constraint by using auxiliary variables $\varepsilon_{T1}(k)$ for every time instance $k \in \{0, \dots, N\}$:

$$\varepsilon_{T1}(k) = \begin{cases} -T_1(k) - \Delta T_1(k) + T_{1,min}, & when\ T_1(k) + \Delta T_1(k) < T_{1,min,} \\ T_1(k) + \Delta T_1(k) - T_{1,max}, & when\ T_1(k) + \Delta T_1(k) > T_{1,max}, \\ 0, & otherwise, \end{cases} \qquad (2.2.18)$$

which are then strongly penalized in the cost function. Since it is not a linear function, the equality is transformed into a group of inequalities

$$\begin{aligned} \varepsilon_{T1}(k) &\geq -T_1(k) - \Delta T_1(k) + T_{1,min}, \\ \varepsilon_{T1}(k) &\geq T_1(k) + \Delta T_1(k) - T_{1,max}, \\ \varepsilon_{T1}(k) &\geq 0. \end{aligned} \qquad (2.2.19)$$

Other constraints are as follows:

- $T_{min} \leq T(k) + \Delta T(k) \leq T_{max}$, to ensure operating conditions of the tank for every layer (not to be confused with operating conditions of the heating circuits). T_{min} and T_{max} are usually found in technical description of the storage tank.

- $|\Delta u(k)| \leq \Delta u_{max}$, to stay in proximity of the linearization point. Δu_{max} boundaries need to be small enough to limit linearization error, but also large enough to come to optimal solution quickly enough. They are set at the beginning of the SLP procedure and decreased every $n_{iter,dcrs}$ iterations to make the programme as quick as possible in the beginning and to reduce oscillations around true optimal point. Every $n_{iter,dcrs}$ maximal power shifts are decreased according to $\Delta u_{max} = \lambda_{\Delta u} \Delta u_{max}$, where $\lambda_{\Delta u} \in \langle 0,1 \rangle$. If the SLP procedure takes many iteration Δu_{max} can become too small, therefore when Δu_{max} falls under a certain threshold, $\Delta u_{max} \leq \Delta u_{max,min}$, the process of decreasing Δu_{max} is stopped.

- $0 \leq u(k) + \Delta u(k) \leq u_{max}$, to stay within heat sources operating limits.

- Expressions to ensure staying in the specific area of operation, which are different for each site as they depend on the state variables and inputs, as well as configuration of the heat storage system and heat sources constraints.

- Additional constraints according to heat sources datasheets and operation guidelines.

Criterion for optimality of the solution refers to KPI_2 – total price of the consumed energy:

$$KPI_2 = c(u + \Delta u), \qquad (2.2.20)$$

where c is a row vector of costs per unit of power within the sampling interval for different elements of the input powers u. KPI_2 is calculated separately from LP since costs from auxiliary variables ε_r and ε_{T1} can be found in total LP cost. SLP is finding a solution with smaller price than in the last iteration, but after some time that drop in price becomes so small that it has no practical gain. To make sure SLP does not get stuck in such situations, a convergence tolerance is set. Current KPI_2 must be smaller than the minimal KPI_2 decreased by the convergence tolerance $conv\_tol$. But the minimal KPI_2 does not have to be the last one. Some local minima can occur during the SLP procedure, so SLP will stop iterating only if KPI_2 did not improve for the last n_{2stop} iterations. Values for n_{2stop} are determined experimentally.

3. Functioning of the energy management tool on the Store4HUC pilot sites

3.1. Croatian pilot site in Bračak

The pilot site in Bračak is an example of a historical urban site where recently significant integration and refurbishment efforts have been already done, making it already now a site with class A energy certificate. Still the site does not have a renewable electricity source or storage and there is no central intelligence which would optimize the system and allow optimal integration of storages and renewable energy. Thus, the investment in Bračak is planned to:

- introduce renewable electrical energy in a form of a photovoltaic plant;

- introduce energy storage in terms of a battery system;

- improve the building automation system and introduce the integration of the IT platform that would induce optimal operation of the newly introduced renewable energy and storages with already existing highly efficient indoor climate control.

The following functionalities of the Store4HUC EMS are envisioned on the Bračak site.

Off-line:

1) planning the optimal investment in and operation of renewable energy source and storage by taking into account yearly energy consumption profiles of the existing HUC setup for different pre-determined return on investment periods, with respected HUC-induced constraints and interactions with the climate control system;

2) autarky rate assessment of the Bračak castle for the selected PV and battery system configuration.

3) planning optimal operation of the combination of wood pellets boiler and micro Combined Heat and Power (CHP) plant which provide heat to the building through a common heat storage, whereas the predicted heat demands of the HUC are respected as well as ensured long-life operation conditions of the mentioned heat sources, coordination with the optimal operation of the battery energy storage system.

On-line:

4) optimal operation of the installed battery energy storage system with the photovoltaic system and the remaining HUC energy-relevant systems, especially the indoor climate control system. It exploits off-line computed results (module (1)) for on-line operation;

5) optimal operation of the combination of wood pellets boiler and micro Combined Heat and Power (CHP) plant which provides heat to the building through a common heat storage, whereas the predicted heat demands of the HUC are respected as well as ensured long-life operation conditions of the mentioned heat sources, coordination with the optimal operation of the battery energy storage system. Ait exploits off-line computed results (module (2)) for on-line operation.

Within this deliverable operation of the modules related to the planned off-line functionality is shown.

3.1.1. Module (1) results for the Bračak pilot site

For Bračak pilot site energy metered at a single point (of total three points) was used, from the year 2018. It is shown in Figure 4. From the same year PV production measurements were used from UNIZGFER PV system. UNIZGFER PV system has $P_{PV,peak,nearby} = 7\ kWp$ and its power profile is depicted in Figure 5.

Power demand profile of Bračak site, P_{dem}
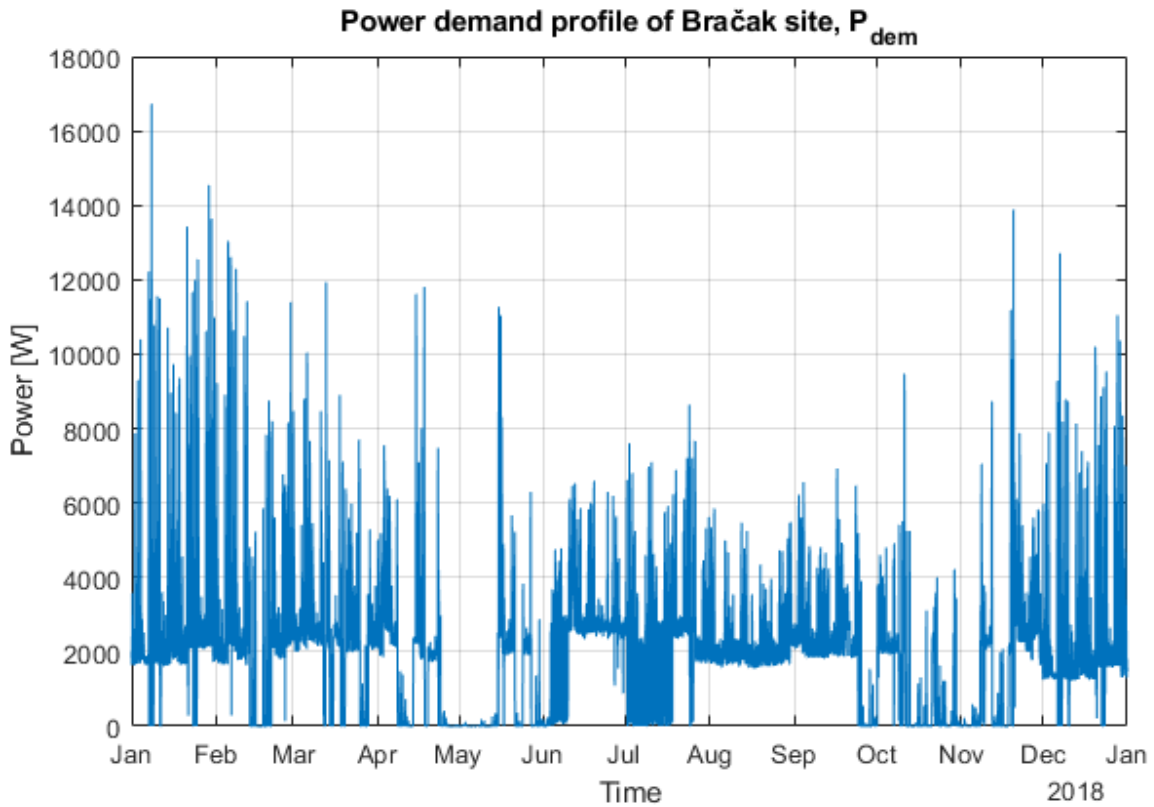
Figure 4. Electrical power demand profile at Bračak site for year 2018.

PV power profile on UNIZGFER, P_{PV}
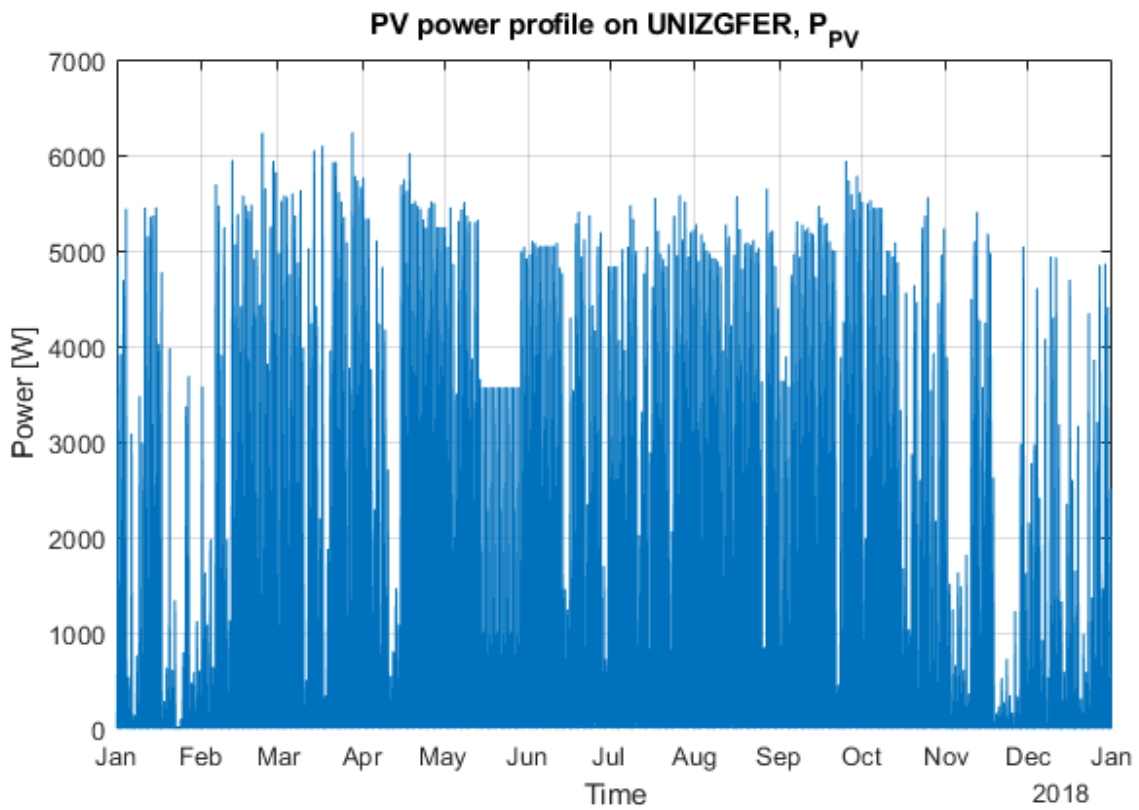
Figure 5. PV power profile at UNIZGFER site for year 2018.

Parameters and prices used for simulation are as follows:

- Battery system parameters
    - Number of cycles (n_{cyc}): 5000
    - Depth of discharge (DoD): 0.8 (80%)
    - Discharging efficiency (η_{dch}): 0.9 (90%)
    - Charging efficiency (η_{ch}): 0.9 (90%)
    - Lifetime of power converter (n_{PC}): 25 years
    - Price of the new battery pack (c_{bat}): 480 €/kWh
    - Price of the new power converter (c_{PC}): 1280 €/kW
    - Prices of the new battery pack and the new power converter are derived from a single price of the whole battery system ($c_{battery\ system}$): 12000 € per 15 kWh storage, and 3.75 kW power converter

- PV panels parameters
    - Peak power of the nearby PV system ($P_{PV,peaknearby}$): 7 kW
    - Maximum PV peak power to be installed ($P_{PV,max}$): 7 kW
    - Lifetime of the PV system (n_{PV}): 25 years
    - Price of the new PV system (c_{PV}): 1.42 €/W

- Grid parameters
    - Maximum power at a single time instance ($P_{dem,max}$): 29.9 kW
    - Cost of electricity (c_{grid}): 0.13 €/kW
    - Cost of peak power monthly ($c_{p,max}$): 5.13 €/kW

Results obtained from simulations are presented in Table 1, Table 2, and Table 3.

Table 1. Optimal PV and battery system sizes for Bračak pilot site, using cost function 1) (KPI₁).

Number of years in which investment must pay off (n_payoff)	10	12	15	20
Battery capacity (E_bat_max) [kWh]	0	0	1.90	5.23
Power converter power (P_pc_max) [kW]	0	0	0.42	1.15
PV system peak power (P_pv) [kWp]	0	1.30	7.00	7.00
Price of el. en. without investment [€]	2970.81	2970.81	2970.81	2970.81
Price of el. en. with investment [€]	2970.81	2742.53	1745.23	1713.88
Price of the investment [€]	0	1850.92	11451.99	13983.50
Price of the investment yearly scaled [€]	0	154.24	763.47	699.17
Price of yearly maintenance [€]	0	74.04	462.11	557.75

Table 2. Optimal PV and battery system sizes for Bračak pilot site, using cost function 2) (KPI₂).

Number of years in which investment must pay off (n_payoff)	10	12	15	20
Battery capacity (E_bat_max) [kWh]	0	0	1.71	5.65
Power converter power (P_pc_max) [kW]	0	0	1.07	2.57
PV system peak power (P_pv) [kWp]	0	1.30	7.00	7.00
Price of el. en. without investment [€]	2970.81	2970.81	2970.81	2970.81
Price of el. en. with investment [€]	2970.81	2742.53	1699.99	1621.80
Price of the investment [€]	0	1850.92	12186.85	15998.50
Price of the investment yearly scaled [€]	0	154.24	812.46	799.92
Price of yearly maintenance [€]	0	74.04	458.37	549.09

Table 3. Optimal PV and battery system sizes for Bračak pilot site, using cost function 3) (KPI₃).

Number of years in which investment must pay off (n_payoff)	10	12	15	20
Battery capacity (E_bat_max) [kWh]	0	0	0	0
Power converter power (P_pc_max) [kW]	0	0	0	0
PV system peak power (P_pv) [kWp]	0	0.52	7.00	7.00
Price of el. en. without investment [€]	2970.81	2970.81	2970.81	2970.81
Price of el. en. with investment [€]	0	2878.70	1761.77	1262.17
Price of the investment [€]	0	743.83	10000.00	10000.00
Price of the investment yearly scaled [€]	0	61.97	666.67	500.00
Price of yearly maintenance [€]	0	29.75	400.00	400.00

Resulted optimal profiles obtained for n_{payoff}=20 and cost function 1 are shown in Figure 6 for the whole year 2018, in Figure 7 for January 2018, and in Figure 8 for August 2018. A detail from the results (August 12th, 2018) is in Figure 9.
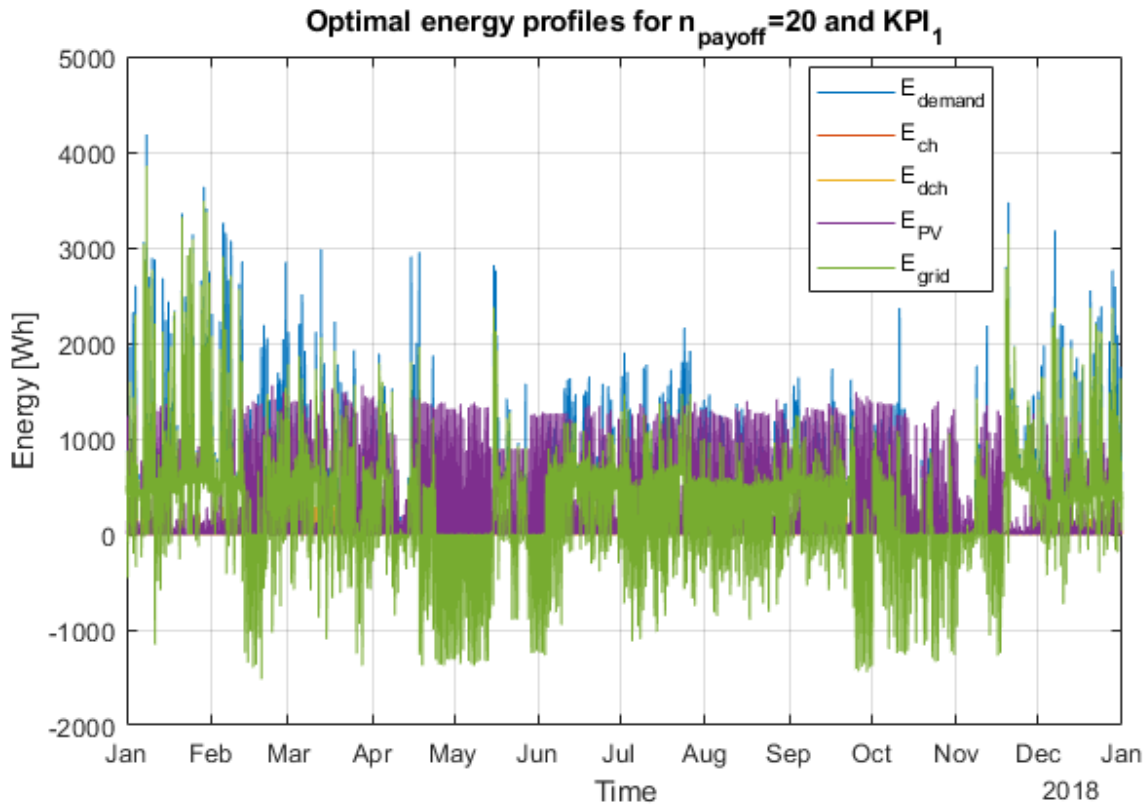
Figure 6. Full optimal energy profiles for Bračak pilot site, obtained for n_{payoff} = 20 and cost function 1. Values on the y-axis represent energy flows during 15 min intervals.
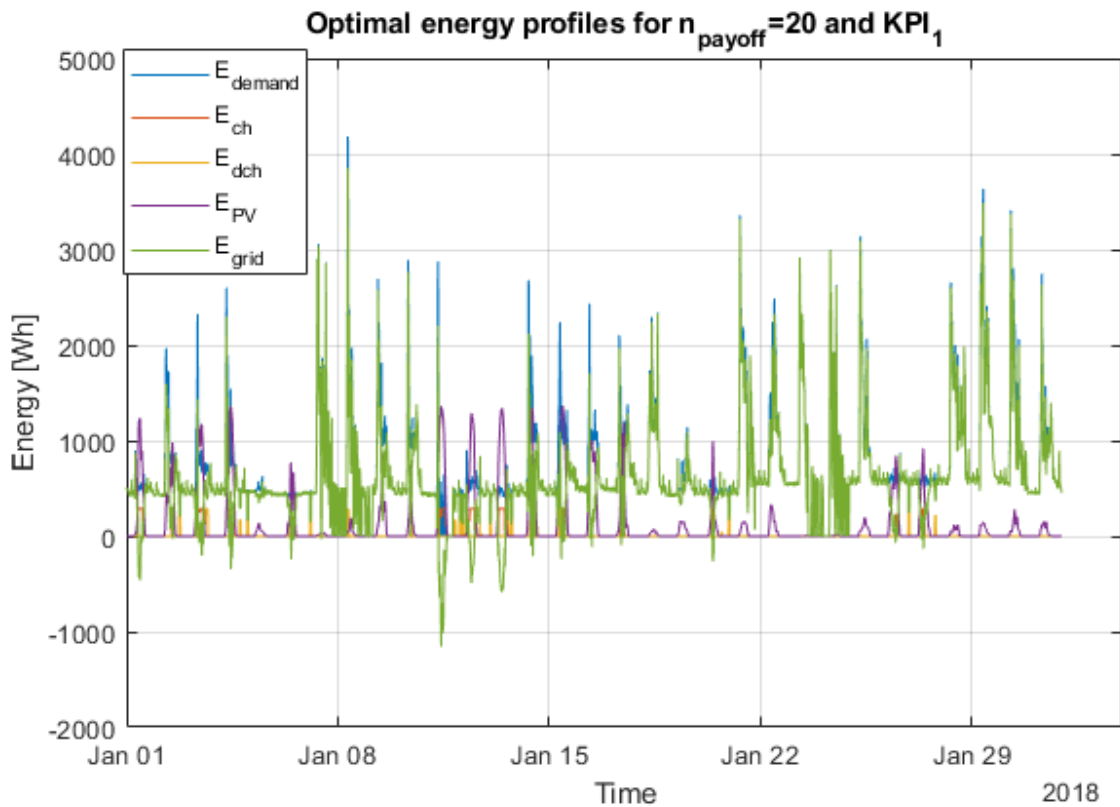
Figure 7. A detail (January 2018) from optimal energy profiles obtained for n_{payoff} = 20 and cost function 1. Values on the y-axis represent energy flows during 15 min intervals.
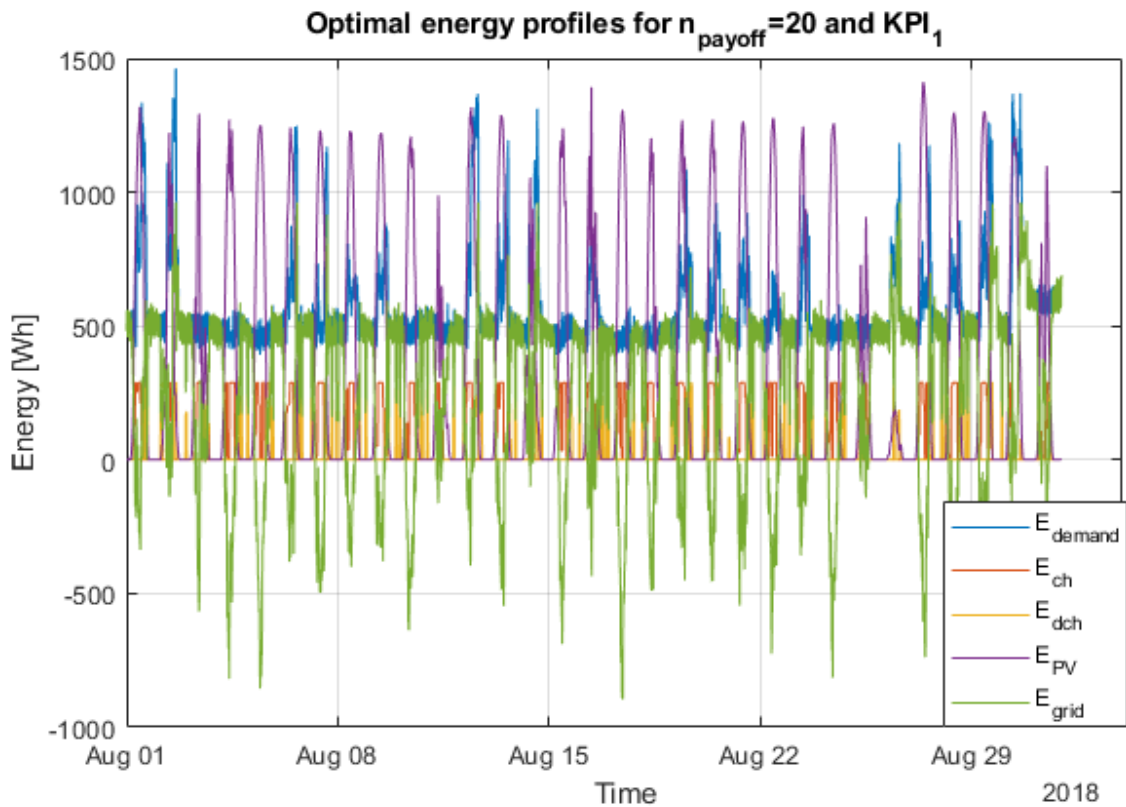
Figure 8. A detail (August 2018) from optimal energy profiles obtained for n_{payoff} = 20 and cost function 1. Values on the y-axis represent energy flows during 15 min intervals.
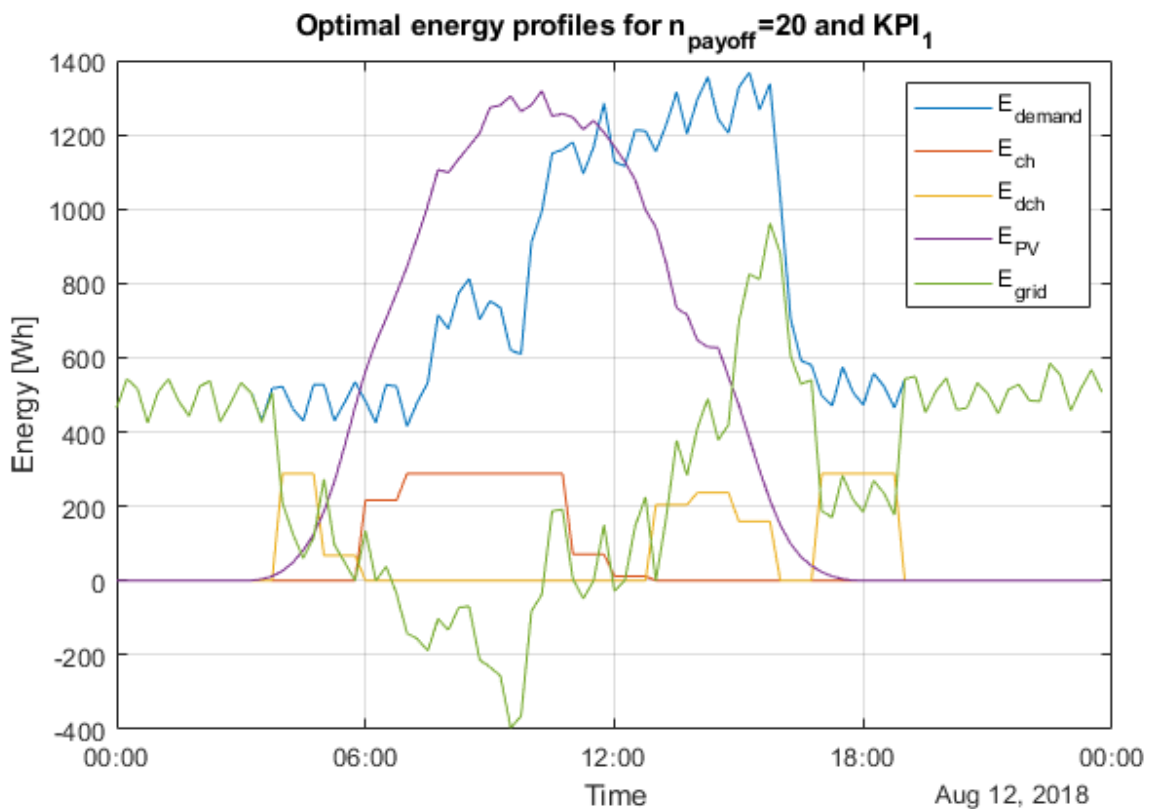
Figure 9. A detail (August 12th, 2018) from optimal energy profiles obtained for n_{payoff} = 20 and cost function 1. Values on the y-axis represent energy flows during 15 min intervals.

3.1.2. Module (2) results for the Bračak pilot site

To demonstrate the results of Module (2), pre-recorded data was used. Since Bračak pilot site does not have correct heating demand measurements, a potential profile is generated using measured heating demand at UNIZGFER from January 17th, 2019. The measured profile was scaled to the size of the Bračak site, any missing data was filled using interpolation, and it was resampled to 15 min sampling time. The final profile is depicted in Figure 10.
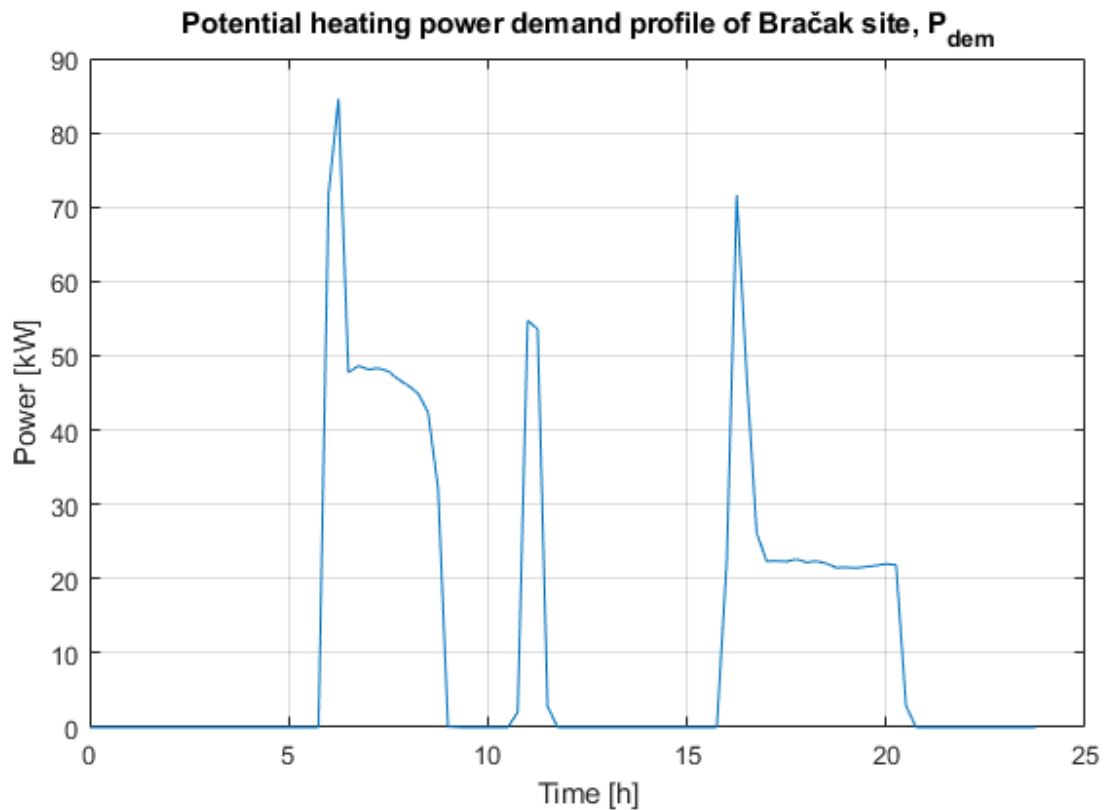
Figure 10. Potential heating power demand profile of Bračak site.

Demand flow profile is generated from the same measurements and it is shown in Figure 11.
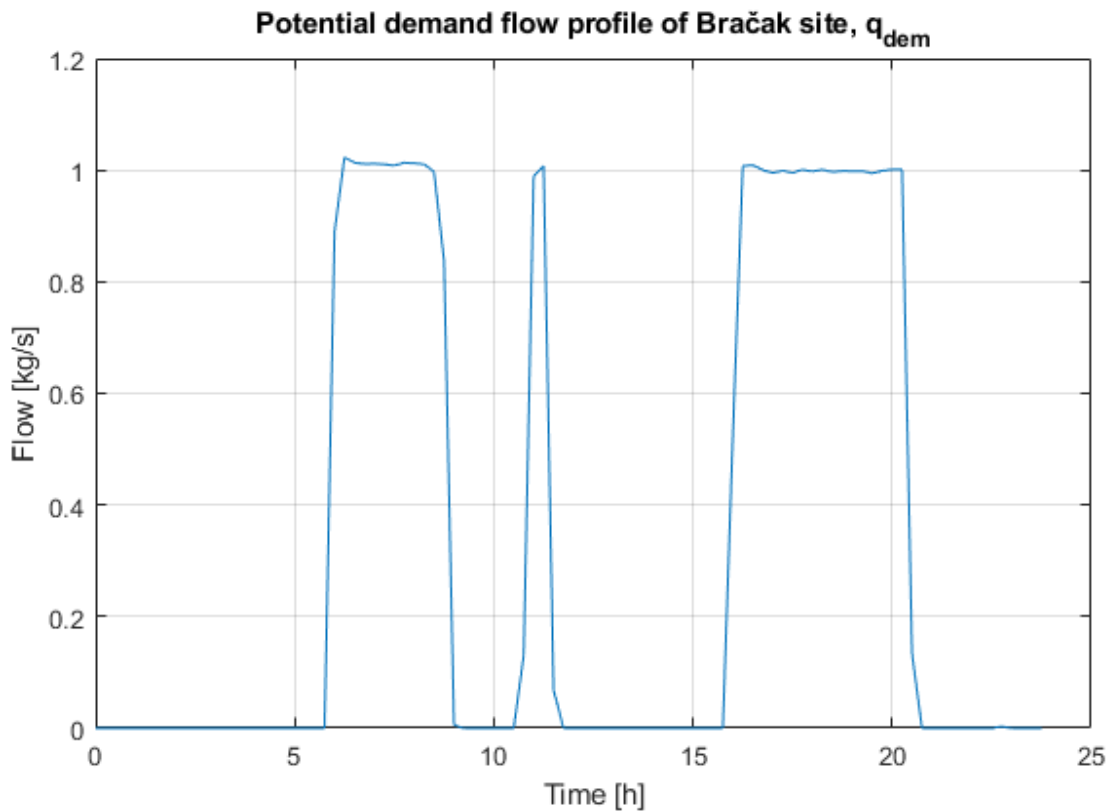
Figure 11. Potential demand flow profile of Bračak site.

The last needed information for the module to work is the temperature of environment air (T_{env}) around the storage tank. Since there are no available measurements for it, and the tank is situated in a boiler room in the basement of the site, it is approximated to be constant at 22°C.

The storage tank itself has a cylindrical shape with height h_{tank} and radius r_{tank}. The heating medium is water. It is stratified to 5 layers, layer 1 being the top one and layer 5 being the bottom one. Mass of water in each layer is calculated as $m_l = r_{tank}^2 \pi h_l \rho_w$, where h_l is the height of the layer l and ρ_w is the density of water. It has 2 available heat sources: combined heat and power (CHP) and wood pellets boiler (WPB). The demand side consists of three heating circuits and two domestic hot water circuits, but, as stated in chapter 2.2, it is simplified to a "black box" where only total power and flow are known. Part of mechanical site drawings regarding the storage tank and the heat sources is shown in Figure 12. The storage tank with marked layers and water supply/return flows is shown in Figure 13.
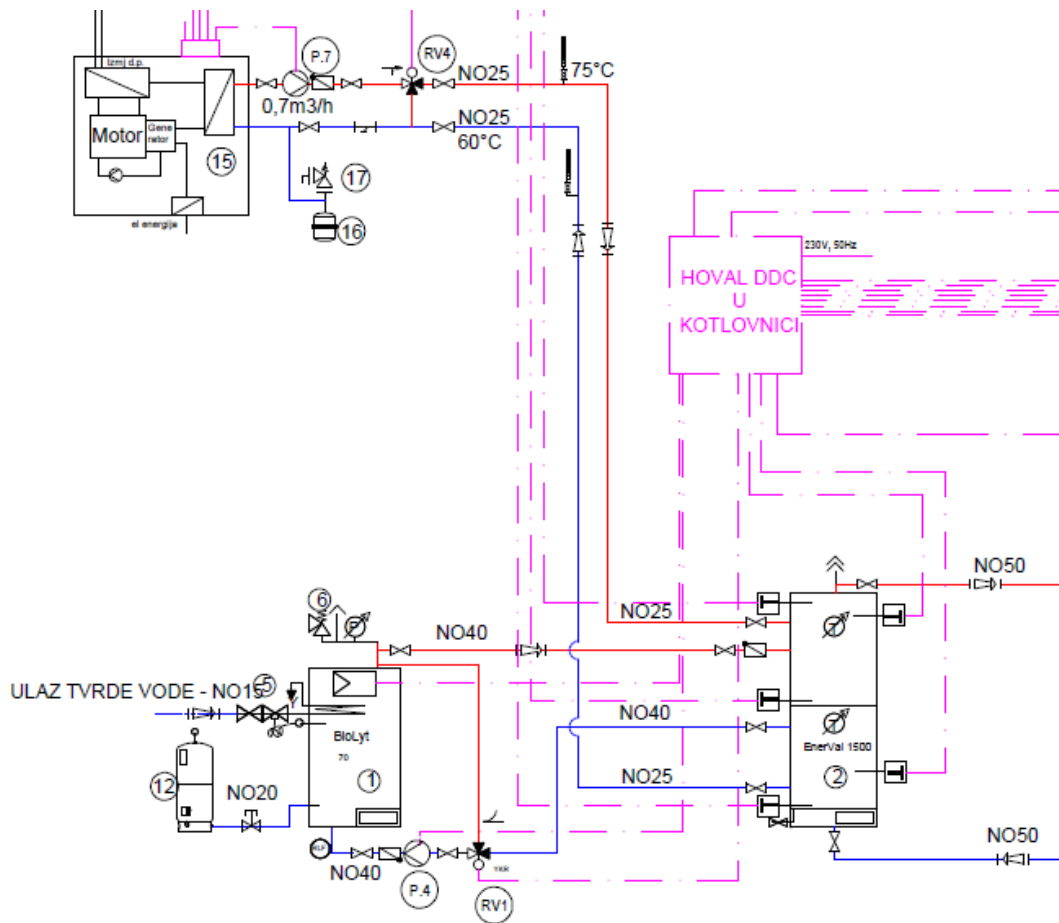
Figure 12. Part of mechanical draft of the Bračak site regarding the storage tank and the heat sources.
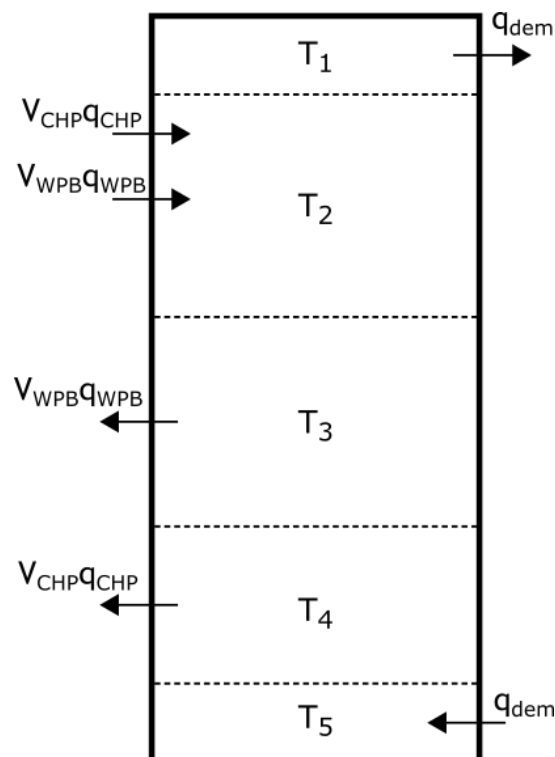
Figure 13. The stratified storage tank at Bračak site.

Following Figure 13 and expressions (2.2.3) – (2.2.6) from chapter 2.2.1, non-linear continuous-time model of the heat storage tank of the Bračak pilot site is:

$$m_1 c_p \frac{d}{dt} T_1 = q_{21} c_p T_2 - q_{12} c_p T_1 - q_{dem} c_p T_1 - (k_c + k_{b12}) \frac{A_h}{\Delta x_{12}} (T_1 - T_2)$$
$$- h A_{w1} (T_1 - T_{env}), \tag{3.1.1}$$

$$m_2 c_p \frac{d}{dt} T_2 = V_{CHP} q_{CHP} c_p \left(T_4 + \frac{P_{CHP}}{V_{CHP} q_{CHP} c_p} \right) + V_{WPB} q_{WPB} c_p \left(T_3 + \frac{P_{WPB}}{V_{WPB} q_{WPB} c_p} \right)$$
$$+ q_{12} c_p T_1 + q_{32} c_p T_3 - q_{21} c_p T_2 - q_{23} c_p T_2$$
$$+ (k_c + k_{b12}) \frac{A_h}{\Delta x_{12}} (T_1 - T_2) - (k_c + k_{b23}) \frac{A_h}{\Delta x_{23}} (T_2 - T_3) \tag{3.1.2}$$
$$- h A_{w2} (T_2 - T_{env}),$$

$$m_3 c_p \frac{d}{dt} T_3 = q_{23} c_p T_2 + q_{43} c_p T_4 - q_{32} c_p T_3 - q_{34} c_p T_3 - V_{WPB} q_{WPB} c_p T_3$$
$$+ (k_c + k_{b23}) \frac{A_h}{\Delta x_{23}} (T_2 - T_3) - (k_c + k_{b34}) \frac{A_h}{\Delta x_{34}} (T_3 - T_4) \tag{3.1.3}$$
$$- h A_{w3} (T_3 - T_{env}),$$

$$m_4 c_p \frac{d}{dt} T_4 = q_{34} c_p T_3 + q_{54} c_p T_5 - q_{43} c_p T_4 - q_{45} c_p T_4 - V_{CHP} q_{CHP} c_p T_4$$
$$+ (k_c + k_{b34}) \frac{A_h}{\Delta x_{34}} (T_3 - T_4) - (k_c + k_{b34}) \frac{A_h}{\Delta x_{45}} (T_4 - T_5) \tag{3.1.4}$$
$$- h A_{w4} (T_4 - T_{env}),$$

$$m_5 c_p \frac{d}{dt} T_5 = q_{45} c_p T_4 - q_{54} c_p T_5 + q_{dem} c_p \left(T_1 - \frac{P_{dem}}{q_{dem} c_p} \right)$$
$$+ (k_c + k_{b45}) \frac{A_h}{\Delta x_{45}} (T_4 - T_5) + h A_{w5} (T_5 - T_{env}). \tag{3.1.5}$$

Furthermore, mass flows between layers are defined as:

$$q_{12} = \max(0, -q_{dem}) = 0 \tag{3.1.6}$$

$$q_{23} = \max(0, V_{CHP} q_{CHP} + V_{WPB} q_{WPB} - q_{dem}) \tag{3.1.7}$$

$$q_{34} = \max(0, V_{CHP} q_{CHP} - q_{dem}) \tag{3.1.8}$$

$$q_{45} = \max(0, -q_{dem}) = 0 \tag{3.1.9}$$

$$q_{54} = \max(0, q_{dem}) = q_{dem} \tag{3.1.10}$$

$$q_{43} = \max(0, q_{dem} - V_{CHP} q_{CHP}) \tag{3.1.11}$$

$$q_{32} = \max(0, q_{dem} - V_{CHP} q_{CHP} - V_{WPB} q_{WPB}) \tag{3.1.12}$$

$$q_{21} = \max(0, q_{dem}) = q_{dem} \tag{3.1.13}$$

Coefficient for buoyant conductivity k_b is calculated in each timestamp as defined in expression (2.2.4) and then used as a constant.

Constraints posed by CHP and WPB are responsible for different dynamics of the system in different areas, i.e. they change expressions for bypass valves V_{CHP} and V_{WPB} respectively. Areas of operation are defined by their minimal input temperatures, $T_{CHP,in,min}$ and $T_{WPB,in,min}$, as well as maximal input temperature for CHP, $T_{CHP,in,max}$. WPB does not have maximal input temperature. Constraints to ensure that the system stays in the current area of operation, i.e. to ensure same system dynamics are:

$$T_4(k) + \Delta T_4(k) < T_{CHP,in,min} \ when \ T_4(k) < T_{CHP,in,min} \tag{3.1.14}$$

$$T_{CHP,in,min} \le T_4(k) + \Delta T_4(k) < T_{CHP,in,max} \ when \ T_{CHP,in,min} \le T_4(k) < T_{CHP,in,max} \tag{3.1.15}$$

$$T_{CHP,in,max} \leq T_4(k) + \Delta T_4(k) \; when \; T_{CHP,in,max} \leq T_4(k) \tag{3.1.16}$$

$$T_3(k) + \Delta T_3(k) < T_{WPB,in,min} \; when \; T_3(k) < T_{WPB,in,min} \tag{3.1.17}$$

$$T_{WPB,in,max} \leq T_3(k) + \Delta T_3(k) \; when \; T_{WPB,in,max} \leq T_3(k) \tag{3.1.18}$$

Dynamics of bypass valves based on areas of operation:

$$V_{CHP} = \begin{cases} 1, when \; T_4 \geq T_{CHP,in,min} \\ \dfrac{P_{CHP}}{P_{CHP} + q_{CHP}c_p\left(T_{CHP,in,min} - T_4\right)}, when \; T_4 < T_{CHP,in,min} \end{cases} \tag{3.1.19}$$

$$V_{WPB} = \begin{cases} 1, when \; T_3 \geq T_{WPB,in,min} \\ \dfrac{P_{WPB}}{P_{WPB} + q_{WPB}c_p\left(T_{WPB,in,min} - T_3\right)}, when \; T_3 < T_{WPB,in,min}. \end{cases} \tag{3.1.20}$$

Maximal input temperature for CHP is responsible for the power CHP can deliver, because $P_{CHP} = 0$ when $T_4 > T_{CHP,in,max}$. When $T_4 \leq T_{CHP,in,max}$ CHP can deliver power according to chart in Figure 14.
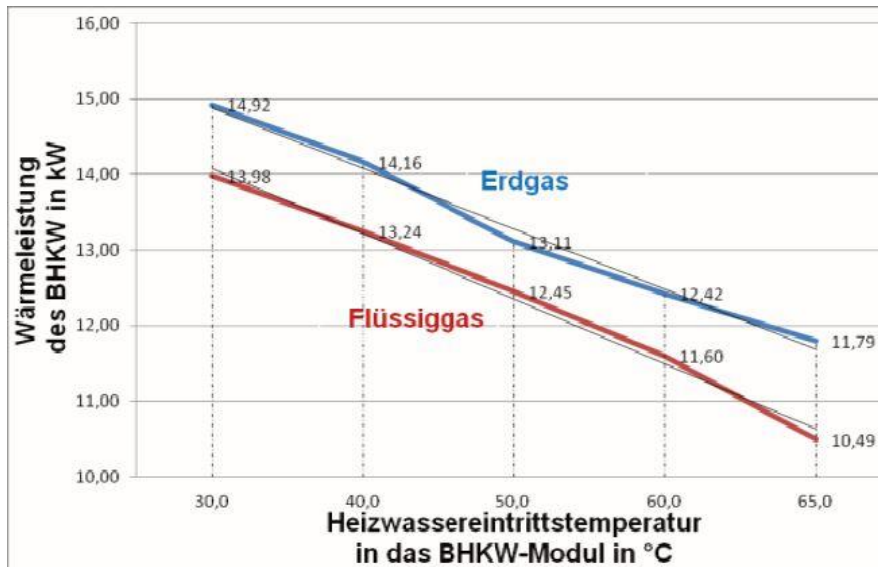
Figure 14. Power profile of CHP depending on input temperature [7].

The CHP uses natural gas as fuel, and its maximal power profile depending on T_4 is charted in Figure 15.
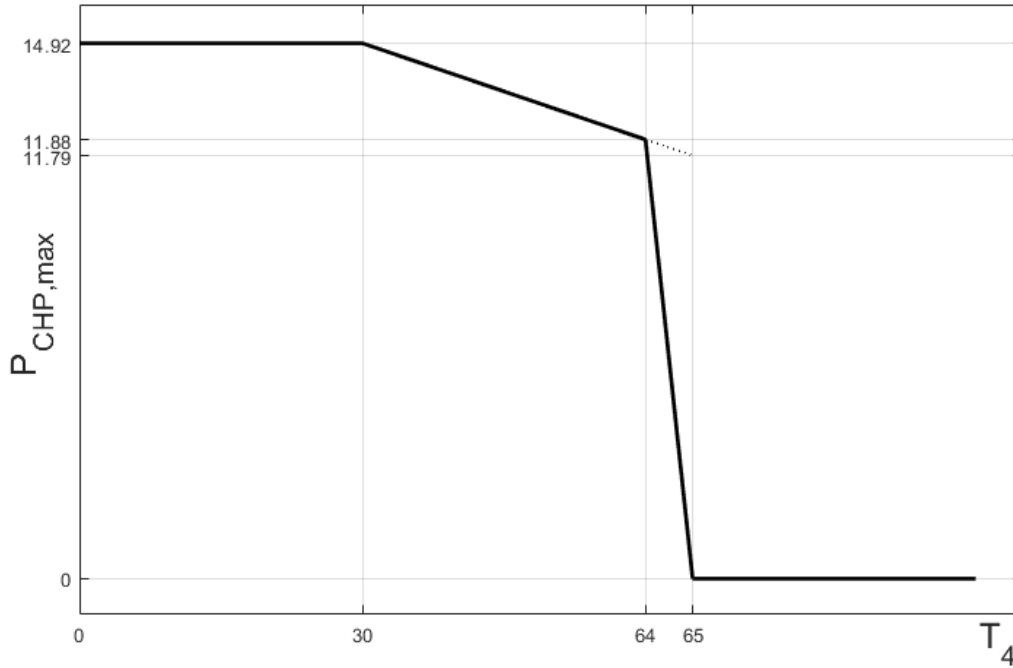
Figure 15. CHP power profile used.

The maximal power between 64 and 65 °C is changed from the original so that the profile is continuous for all possible values of T_4. These power constraints on CHP written in a form suitable for a LP are:

$$when\ T_4 \le T_{CHP,in,min}: \begin{cases} P_{CHP} \le P_{CHP,max} \\ P_{CHP} \le k_2 T_4 + l_2, \\ P_{CHP} \le k_3 T_4 + l_3 \end{cases} \tag{3.1.21}$$

$$when\ T_4 > T_{CHP,in,max}:\ P_{CHP} \le 0, \tag{3.1.22}$$

where k_2, l_2, k_3 and l_3 are calculated using equation for the line through two given points.

Initial conditions for temperatures are chosen to be 70 °C for all layers, i.e. $T_1(0) = T_2(0) = T_3(0) = T_4(0) = T_5(0) = 70\ °C$. Initial power profiles are chosen to be equal to the power demand profile, all coming from WPB since rated power of CHP is significantly lower than the required thermal power. Moreover, current control scheme of the heat sources in the Bračak site uses the WPB as a primary and the CHP as a secondary source.

Price for using WPB per unit of power in one sampling interval c_{WPB} [€/W] is calculated using a general price of wood pellets c_{pel} [€/kg], specified efficiency of the WPB η_{WPB}, and mass of pellets per unit of energy m_{pel} [kg/Ws]:

$$c_{WPB} = \frac{1}{\eta_{WPB}} m_{pel} c_{pel} T_s. \tag{3.1.23}$$

Price for using CHP per unit of power in one sampling interval [€/W] is somewhat more complex because the price of the burned gas is reduced by the price of electricity CHP has generated. Moreover, Bračak site has 2 tariff prices for electricity so CHP has different prices for day and night. The formula for CHP pricing in tariff t is:

$$c_{CHP,t} = \left(\frac{1}{\eta_{CHP,th}} c_{gas} - \frac{\eta_{CHP,el}}{\eta_{CHP,th}} c_{el,t} \right) T_s, \tag{3.1.24}$$

where $\eta_{CHP,th}$ is the CHP's thermal efficiency, $\eta_{CHP,el}$ is the CHP's electrical efficiency, c_{gas} is the price of natural gas per unit of energy, and $c_{el,t}$ is the price of electricity in tariff t. Day tariff is active from 7:00 to 21:00, while night tariff is active from 21:00 to 7:00.

Finally, values of constants, parameters, sizes, and prices used in the simulation are:

- constants:
  - density of water, $\rho_w = 986.7 \, \text{kg/m}^3$,
  - specific heat capacity of water, $c_p = 4185.1 \, \text{J/(kg K)}$,
  - thermal expansion coefficient of water, $\alpha_p = 0.516 \cdot 10^{-3} \, \text{K}^{-1}$,
  - von Karman constant, $\kappa = 0.41$,
  - water conductivity coefficient, $k_c = 0.637095 \, \text{W/(m K)}$,
  - heat transfer coefficient, $h = 0.2068 \, \text{W/(m}^2 \, \text{K)}$,
- storage tank dimensions:
  - radius of the tank, $r_{tank} = 0.5 \, \text{m}$,
  - total height of the tank, $h_{tank} = 2 \, \text{m}$,
  - height of layer 1, $h_1 = 0.2 \, \text{m}$,
  - height of layer 2, $h_2 = 0.6 \, \text{m}$,
  - height of layer 3, $h_3 = 0.6 \, \text{m}$,
  - height of layer 4, $h_4 = 0.4 \, \text{m}$,
  - height of layer 5, $h_5 = 0.2 \, \text{m}$,
  - length between midpoints of layers 1 and 2, $\Delta x_{12} = 0.4 \, \text{m}$,
  - length between midpoints of layers 2 and 3, $\Delta x_{23} = 0.6 \, \text{m}$,
  - length between midpoints of layers 3 and 4, $\Delta x_{34} = 0.5 \, \text{m}$,
  - length between midpoints of layers 4 and 5, $\Delta x_{45} = 0.3 \, \text{m}$,
  - thickness of the insulation, $d_i = 0.12 \, \text{m}$;
- operating parameters:
  - minimal outlet temperature, $T_{1,min} = 60 \, °\text{C}$,
  - maximal outlet temperature, $T_{1,max} = 80 \, °\text{C}$,
  - maximal temperature of water in the tank, $T_{max} = 95 \, °\text{C}$,
  - minimal input temperature in the CHP unit, $T_{CHP,in,min} = 30 \, °\text{C}$,
  - maximal input temperature in the CHP unit, $T_{CHP,in,max} = 65 \, °\text{C}$,
  - minimal input temperature in the WPB unit, $T_{WPB,in,min} = 65 \, °\text{C}$,
  - maximal input temperature in the WPB unit, $T_{WPB,in,max} = 95 \, °\text{C}$ (there is no such value specified by the manufacturer),
  - maximal CHP unit thermal power $P_{CHP,max} = 14.92 \, \text{kW}$,
  - maximal WPB thermal power $P_{WPB,max} = 80 \, \text{kW}$,
  - mass flow of the CHP pump, $q_{CHP} = 0.1919 \, \text{kg/s}$,
  - mass flow of the WPB pump, $q_{WPB} = 0.1919 \, \text{kg/s}$,
- optimization procedure parameters:

- maximal shift in power for CHP, $\Delta P_{CHP,max} = 500\,\text{W}$,

- maximal shift in power for WPB, $\Delta P_{WPB,max} = 500\,\text{W}$,

- convergence tolerance, $conv_{tol} = 0.0013€$ (0.01 kn),

- number of non-improved iterations before stopping, $n_{2stop} = 10$,

- number of iterations before decreasing maximal shifts in power, $n_{iter,dcrs} = 50$

- coefficient of Δu_{max} decrease, $\lambda_{\Delta u} = 0.8$;

- prices:

  - price of wood pellets, $c_{pel} = 0.2649\,€/\text{kg}$ (2 kn/kg),

  - mass of wood pellets per unit of energy, $m_{pel} = 1\,\text{kg/kWh} = 5.5556 \cdot 10^{-8}\,\text{kg/Ws}$,

  - efficiency of WPB, $\eta_{WPB} = 0.95$,

  - price of natural gas, $c_{gas} = 0.2443\,\text{kn/kWh} = 8.9882 \cdot 10^{-9}\,€/\text{Ws}$,

  - price of electricity for day tariff, $c_{el,day} = 0.9727\,\text{kn/kWh} = 3.5787 \cdot 10^{-8}\,€/\text{Ws}$,

  - price of electricity for day tariff, $c_{el,night} = 0.5919\,\text{kn/kWh} = 2.1777 \cdot 10^{-8}\,€/\text{Ws}$,

  - conversion rate HRK to EUR, $1\,€ = 7.55\,kn$.

With such parameters and prices, cost of running the CHP during the day is negative because of high difference in price between electrical energy and natural gas. That is the reason SLP will use CHP power to the maximum during the day.

The SLP procedure yielded optimal results after 143 iterations. Initial power profiles are shown in Figure 16, initial temperature profiles are shown in Figure 17, optimal power profiles are shown in Figure 18, and optimal temperature profiles in Figure 19.
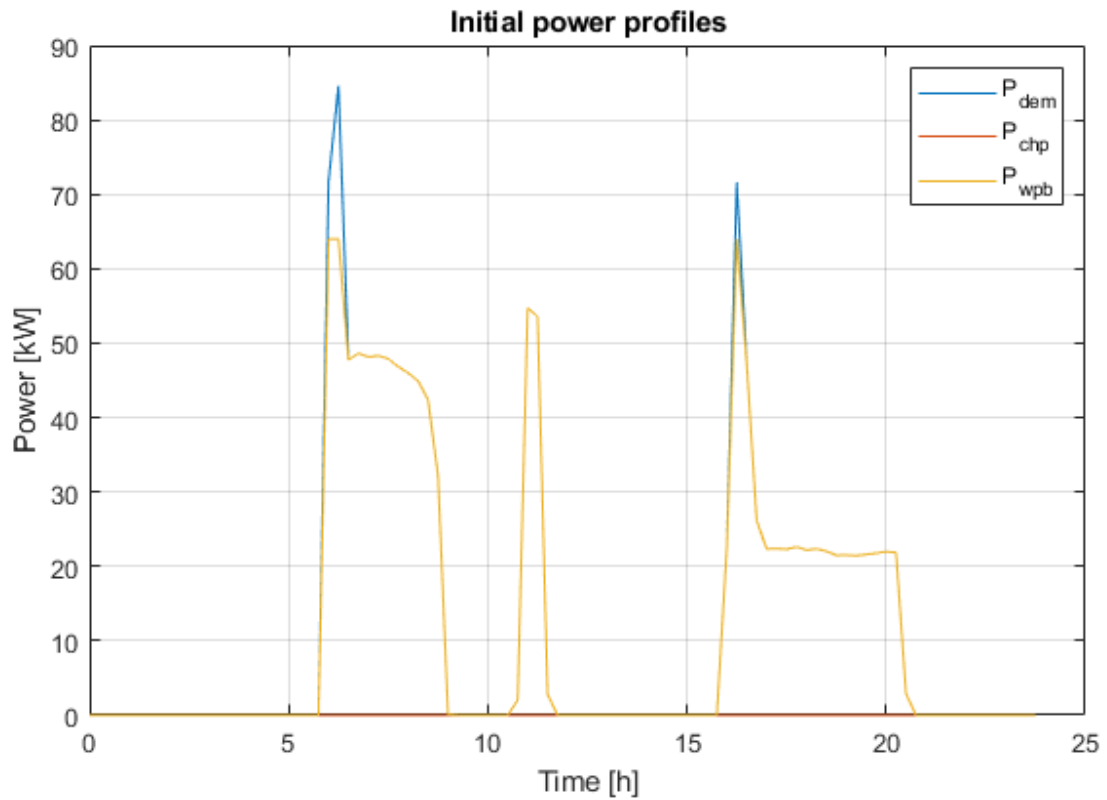
Figure 16. Power profiles of the storage tank in the Bračak site in initial conditions.
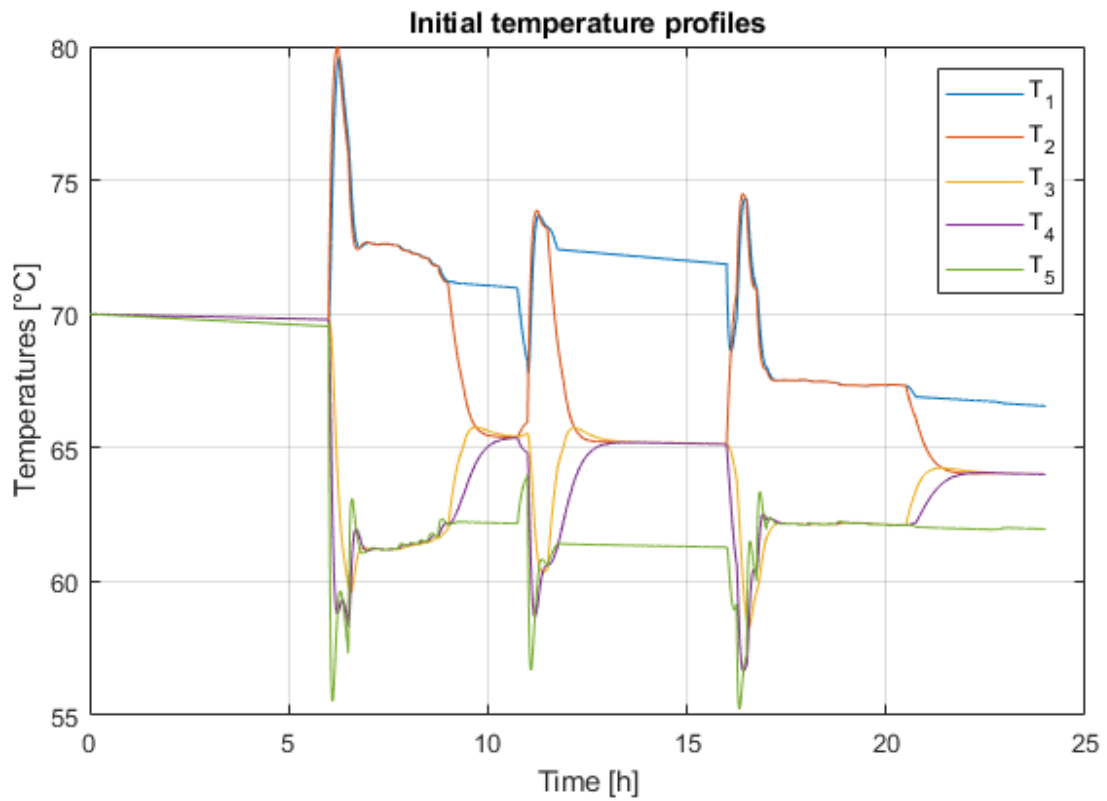
Figure 17. Temperature profiles of the storage tank in the Bračak site in initial conditions.
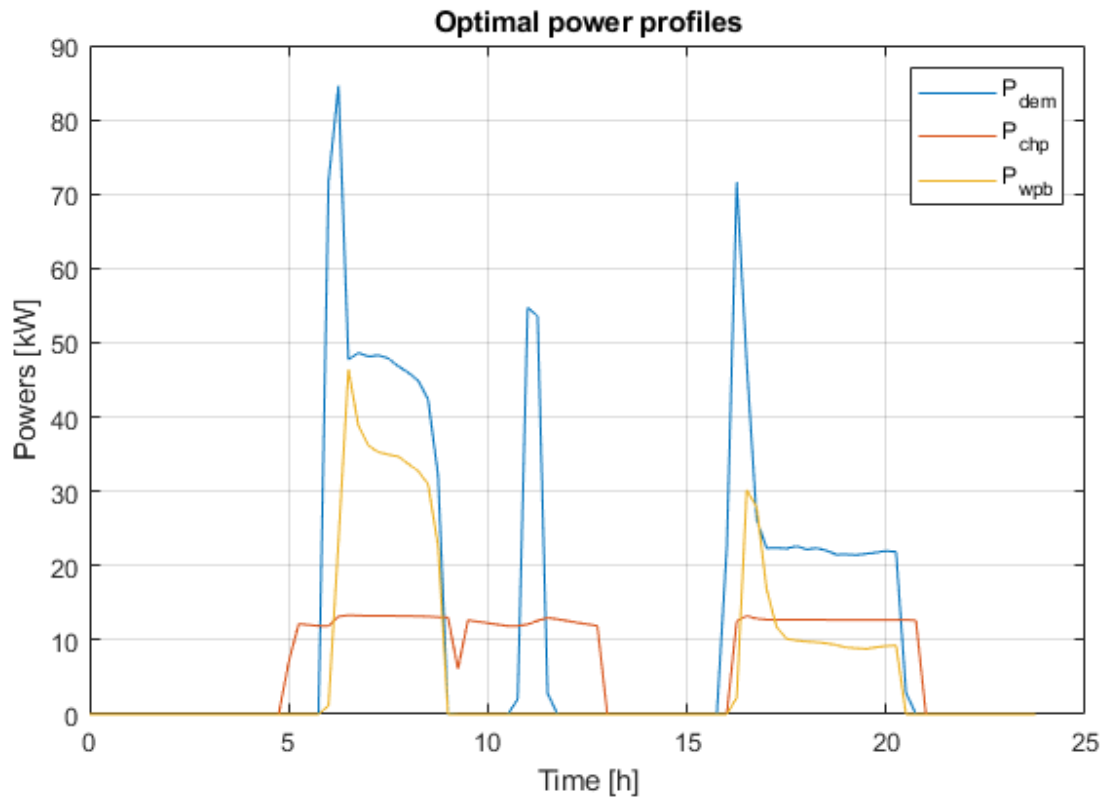
Figure 18. Optimal power profiles of the storage tank in the Bračak site.
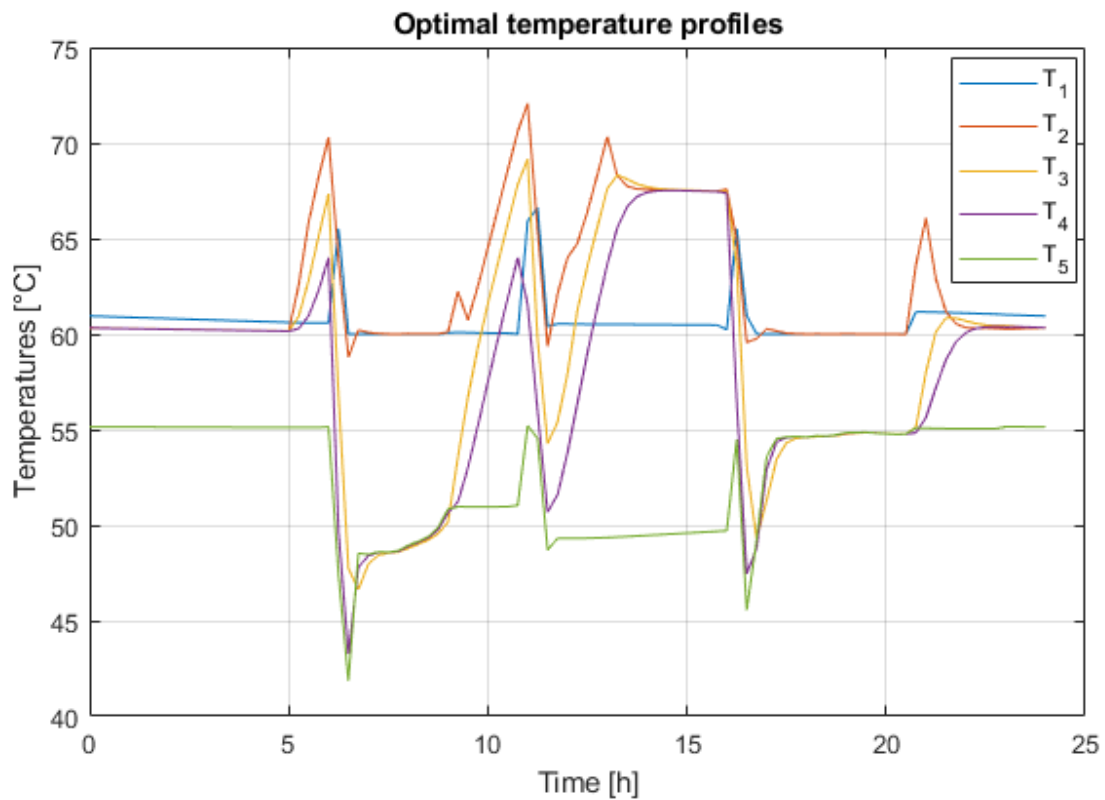
Figure 19. Optimal temperature profiles of the storage tank in the Bračak site.

If initial conditions of this SLP are considered as an estimate of the current control scheme, then the price of heating sequence for given day in current conditions would be 14.75 €. The daily price of heating sequence calculated by module 2 would be 6.68 €, which represents a huge cost reduction, by more than 54%. However, this is a simulation with estimated values used and the results in real world would be different, but it is a good indicator of the module's positive impact on reduction of heating costs.

There are some more constraints on CHP and WPB not yet modelled. They both have a minimal power they can deliver if they are switched on. Looking at Figure 18, it does not seem to be a problem for CHP since its power is always at the maximum, which is expected because of its negative price during the day. On the other hand, minimal operating power of WPB is $P_{WPB,min} = 24\,\text{kW}$ which is more than any $P_{WPB}(t)$ where t is from approximately 15 to 20 h. Another problem for both heat sources is minimal time of operation. Once turned on, CHP must be running for at least 3 hours. There is no such defined time for WPB, but it also should not be turned on and off too frequently. Both problems will be resolved in the course of implementation of the module on the Bračak site in the course of the project.

3.2. Italian pilot site in Cuneo

The sloping elevator in Cuneo is planned to be equipped with a battery storage and a PV system.

The EMS tool should in this case decide what would be the optimal investment in terms of battery and PV system capacities as well as the optimized behaviour of the battery storage system considering a longer-term recorded electricity consumption of the sloping elevator. The battery system efficiency, its degradation characteristics and price, and the pricing conditions of electricity towards the grid will be taken into account.

The typical electricity demands for the elevator after the investment are assessed for working days, Saturdays, Sundays and holidays and then extrapolated for the whole year period.

The following functionalities of the Store4HUC EMS are envisioned on the Cuneo site.

Off-line:

1) planning the optimal investment in and operation of renewable energy source and storage by taking into account yearly energy consumption profiles of the existing HUC set-up for different pre-determined return on investment periods, with respected HUC-induced constraints;

Thus module (1) is applied on the Cuneo site.

3.2.1. Module (1) results for the Cuneo pilot site

For Cuneo pilot site energy metered on a typical working day, a typical Saturday and a typical Sunday was used. Firstly, the data is extrapolated to a full year, considering consumption on Italian national holidays same as on Sundays. The plan for Cuneo pilot is to install bidirectional power converter for the sloping elevator which is able to return energy from the elevator if it is descending under load or ascending without load. With such configuration it is estimated that the new power consumption will be reduced to about 30% of the original value. Therefore, the full energy profile is then multiplied by a factor of 0.3. Estimated yearly energy profile is shown in Figure 20, while the typical weekly profile is shown in Figure 21.
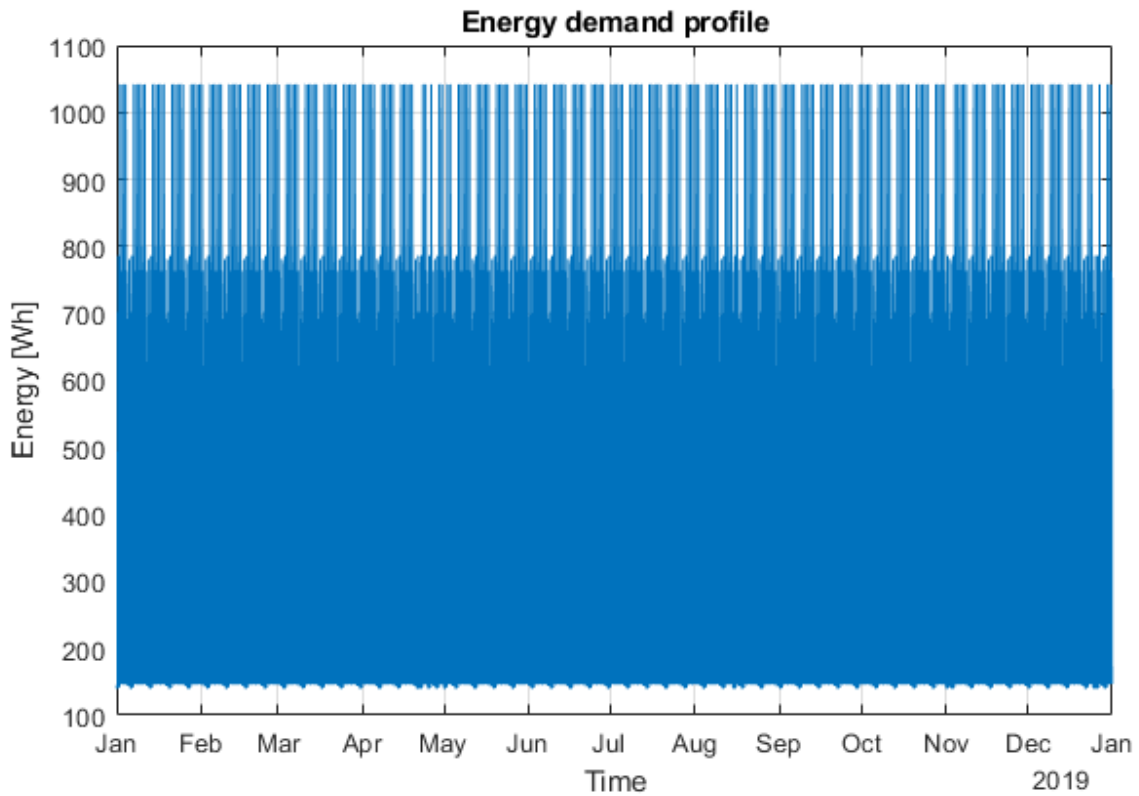
Figure 20. Estimated yearly energy demand of pilot site in Cuneo. Values on the y-axis represent energy flows during 1 h intervals.
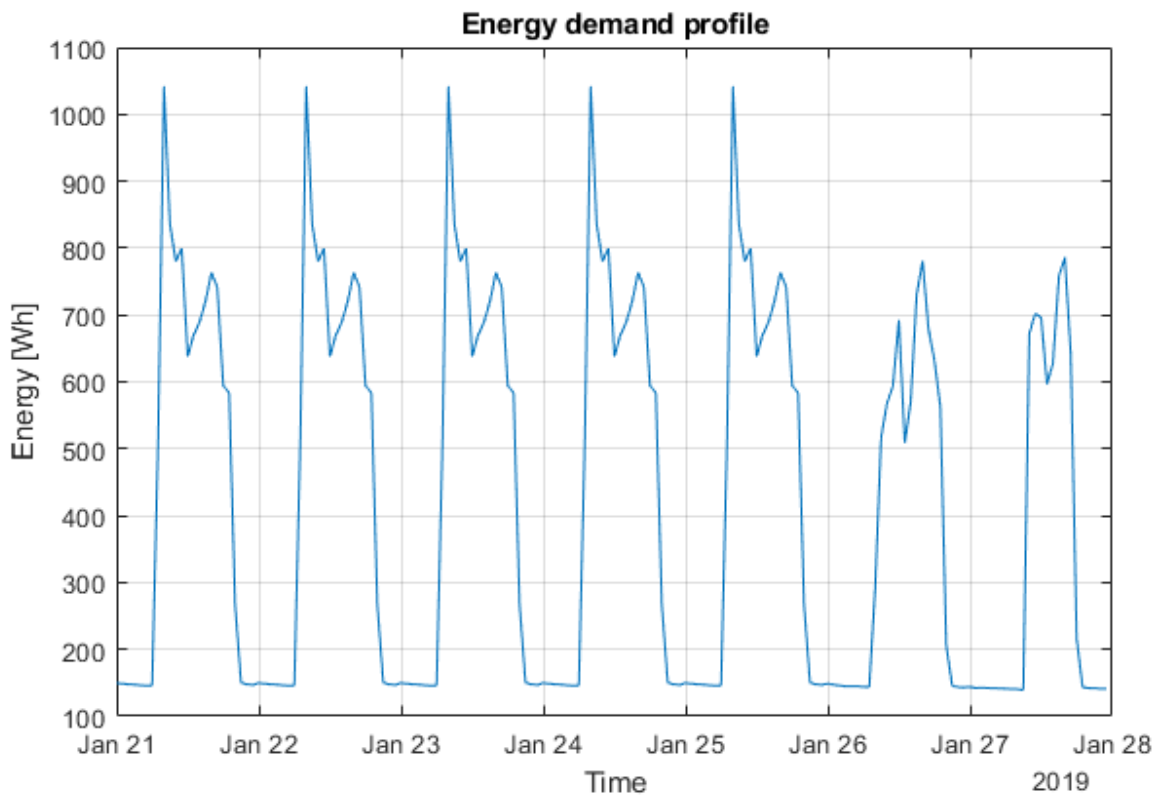
Figure 21. Estimated weekly energy demand of pilot site in Cuneo. Values on the y-axis represent energy flows during 1 h intervals.

Unlike for Croatian pilot Bračak where peak power is measured as mean power in 15 min periods, peak power for pilot in Cuneo is measured every second. If every second in a year was modelled, the LP problem would have been too large to be solved on a regular computer. Therefore, a simplification is introduced. The data was sampled to 1-h increments, and the resulting power of those 1-h increments is multiplied by a factor β_{peak} to be as close as possible to the real power. This β_{peak} is calculated as:

$$\beta_{peak} = \frac{mean(P_{demand,real})}{mean(P_{demand,resampled})}. \tag{3.2.1}$$

For the solar power profile, the same one as for the Bračak module was used. Measurements were used from UNIZGFER PV system with $P_{PV,peak,nearby} = 7$ kWp. Its power profile is depicted in Figure 5.

Furthermore, for Cuneo pilot this module is adapted to include nonlinear pricing of energy being fed into the grid. The formula for pricing of feed-in energy is:

$$J_{feed} = \min\left(c_{feed1} \sum_{k=0}^{N-1} E_{g,pos}, c_{feed2} \sum_{k=0}^{N-1} E_{g,neg} \right) \\ + c_{feed3} \min\left(\sum_{k=0}^{N-1} E_{g,pos}, \sum_{k=0}^{N-1} E_{g,neg} \right), \tag{3.2.2}$$

where $E_{g,neg}$ is the negative part of the grid energy, i.e. energy fed into the grid. Both $E_{g,neg}$ and J_{feed} are included in the optimization vector x. Energy fed into the grid is defined as:

$$E_{g,neg}(k) = \max\left(0, -E_{grid}(k) \right). \tag{3.2.3}$$

Parameters and prices used for simulation are as follows:

- Battery system parameters
    - Number of cycles (n_{cyc}): 5000
    - Depth of discharge (DoD): 0.8 (80%)
    - Discharging efficiency (η_{dch}): 0.9 (90%)
    - Charging efficiency (η_{ch}): 0.9 (90%)
    - Lifetime of power converter (n_{PC}): 25 years
    - Price of the new battery pack (c_{bat}): 480 €/kWh
    - Price of the new power converter (c_{PC}): 1280 €/kW
    - Prices of the new battery pack and the new power converter are derived from a single price of the whole battery system ($c_{battery\ system}$): 12000 € per 15 kWh storage, and 3.75 kW power converter
- PV panels parameters
    - Peak power of the nearby PV system ($P_{PV,peaknearby}$): 7 kW
    - Maximum PV peak power to be installed -- HUC constraint ($P_{PV,max}$): 10 kW
    - Lifetime of the PV system (n_{PV}): 25 years
    - Price of the new PV system (c_{PV}): 1 €/W
- Grid parameters
    - Cost of electricity (c_{grid}): 0.176 €/kW
    - Cost of peak power monthly ($c_{p,max}$): 4.925 €/kW

- Feed-in energy cost 1 (c_{feed1}): 0.08 €/kWh

- Feed-in energy cost 2 (c_{feed2}): 0.07 €/kWh

- Feed-in energy cost 3 (c_{feed3}): 0.06 €/kWh

Results obtained from simulations for different return on investment periods and different optimality criterions are presented in Table 4, Table 5, Table 6 and Table 7.

Table 4. Optimal PV and battery system sizes for Cuneo pilot site, along with simulated energy and price values, for return on investment period of 10 years.

Optimality criterion	Overall energy taken from the grid, KPI1	Price of the overall energy taken from the grid, KPI2	Price of the overall energy taken from the grid + price of the investment yearly scaled + price of the yearly maintenance
Battery capacity (E_bat_max) [kWh]	6.05	6.93	0.82
Power converter power (P_pc_max) [kW]	0.76	0.74	0.34
PV system peak power (P_pv) [kWp]	3.79	3.58	1.20
Overall energy demand [kWh]	3745.10	3745.10	3745.10
Energy taken from the grid (KPI1) [kWh]	963.03	991.05	2416.62
Energy fed into the grid [kWh]	1514.93	1277.68	83.72
Price of el. en. without investment [€]	1361.60	1361.60	1361.60
Price of el. en. with investment (KPI2) [€]	253.22	237.19	873.17
Price of the investment [€]	7668.98	7855.19	2035.87
Price of the investment yearly scaled [€]	766.90	785.52	203.59
Price of yearly maintenance [€]	341.48	338.89	85.46
Yearly saving for the first 10 years [€]	0.00	0.00	199.38
Yearly saving after the first 10 years [€]	766.90	785.52	402.97
Peak power avg. [kW]	3.54	3.24	7.58

Table 5. Optimal PV and battery system sizes for Cuneo pilot site, along with simulated energy and price values, for return on investment period of 12 years.

Optimality criterion	Overall energy taken from the grid, KPI1	Price of the overall energy taken from the grid, KPI2	Price of the overall energy taken from the grid + price of the investment yearly scaled + price of the yearly maintenance
Battery capacity (E_bat_max) [kWh]	6.70	8.21	0.95
Power converter power (P_pc_max) [kW]	0.91	0.87	0.35
PV system peak power (P_pv) [kWp]	4.61	4.26	1.29
Overall energy demand [kWh]	3745.10	3745.10	3745.10
Energy taken from the grid (KPI1) [kWh]	792.30	821.11	2337.41
Energy fed into the grid [kWh]	2318.50	1915.12	105.29

Price of el. en. without investment [€]	1361.60	1361.60	1361.60
Price of el. en. with investment (KPI2) [€]	220.85	203.10	848.76
Price of the investment [€]	8997.20	9323.94	2204.20
Price of the investment yearly scaled [€]	749.77	776.99	183.68
Price of yearly maintenance [€]	390.98	381.51	94.45
Yearly saving for the first 12 years [€]	0.00	0.00	234.71
Yearly saving after the first 12 years [€]	749.77	776.99	418.39
Peak power avg. [kW]	3.12	2.80	7.40

Table 6. Optimal PV and battery system sizes for Cuneo pilot site, along with simulated energy and price values, for return on investment period of 15 years.

Optimality criterion	Overall energy taken from the grid, KPI1	Price of the overall energy taken from the grid, KPI2	Price of the overall energy taken from the grid + price of the investment yearly scaled + price of the yearly maintenance
Battery capacity (E_bat_max) [kWh]	8.06	10.51	1.66
Power converter power (P_pc_max) [kW]	1.09	1.02	0.43
PV system peak power (P_pv) [kWp]	5.67	5.17	1.50
Overall energy demand [kWh]	3745.10	3745.10	3745.10
Energy taken from the grid (KPI1) [kWh]	622.73	646.33	2150.26
Energy fed into the grid [kWh]	3411.13	2818.67	140.06
Price of el. en. without investment [€]	1361.60	1361.60	1361.60
Price of el. en. with investment (KPI2) [€]	180.51	159.22	772.04
Price of the investment [€]	10939.38	11517.18	2851.03
Price of the investment yearly scaled [€]	729.29	767.81	190.07
Price of yearly maintenance [€]	451.80	434.57	124.09
Yearly saving for the first 15 years [€]	0.00	0.00	275.40
Yearly saving after the first 15 years [€]	729.29	767.81	465.47
Peak power avg. [kW]	2.57	2.19	6.66

Table 7. Optimal PV and battery system sizes for Cuneo pilot site, along with simulated energy and price values, for return on investment period of 20 years.

Optimality criterion	Overall energy taken from the grid, KPI1	Price of the overall energy taken from the grid, KPI2	Price of the overall energy taken from the grid + price of the investment yearly scaled + price of the yearly maintenance
Battery capacity (E_bat_max) [kWh]	11.67	13.88	3.89
Power converter power (P_pc_max) [kW]	1.44	1.31	0.57

PV system peak power (P_pv) [kWp]	6.83	6.51	1.94
Overall energy demand [kWh]	3745.10	3745.10	3745.10
Energy taken from the grid (KPI1) [kWh]	429.08	444.23	1739.80
Energy fed into the grid [kWh]	4578.21	4211.12	159.69
Price of el. en. without investment [€]	1361.60	1361.60	1361.60
Price of el. en. with investment (KPI2) [€]	115.53	104.19	596.99
Price of the investment [€]	14274.33	14848.03	4537.55
Price of the investment yearly scaled [€]	713.72	742.40	226.88
Price of yearly maintenance [€]	532.35	515.01	203.99
Yearly saving for the first 20 years [€]	0.00	0.00	333.74
Yearly saving after the first 20 years [€]	713.72	742.40	560.62
Peak power avg. [kW]	1.62	1.42	4.92

Resulted optimal profiles obtained for n_{payoff}=20 and cost function 1 (KPI$_1$) are shown in Figure 22 for the whole year, in Figure 23 for January, and in Figure 24 for August. A detail from the results (August 12th) is in Figure 25.
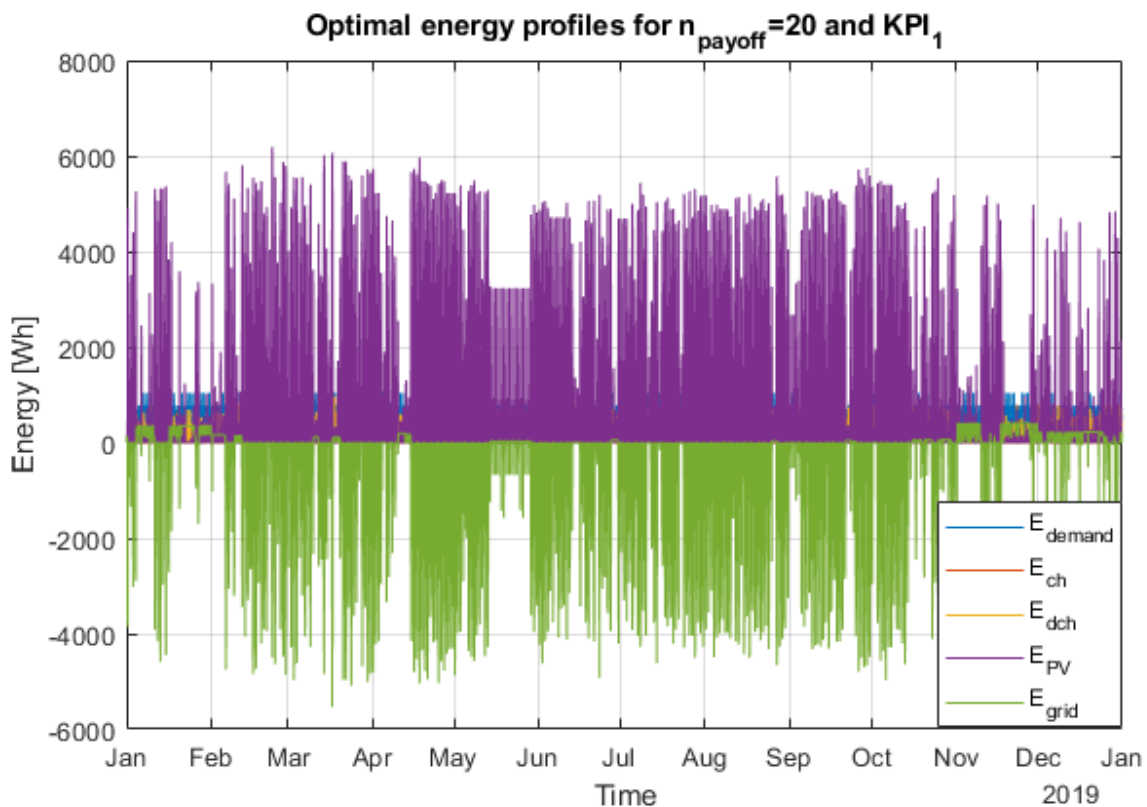
Figure 22. Full optimal energy profiles for Cuneo pilot site, obtained for $n_{payoff} = 20$ and cost function 1 (KPI$_1$). Values on the y-axis represent energy flows during 1 h intervals.
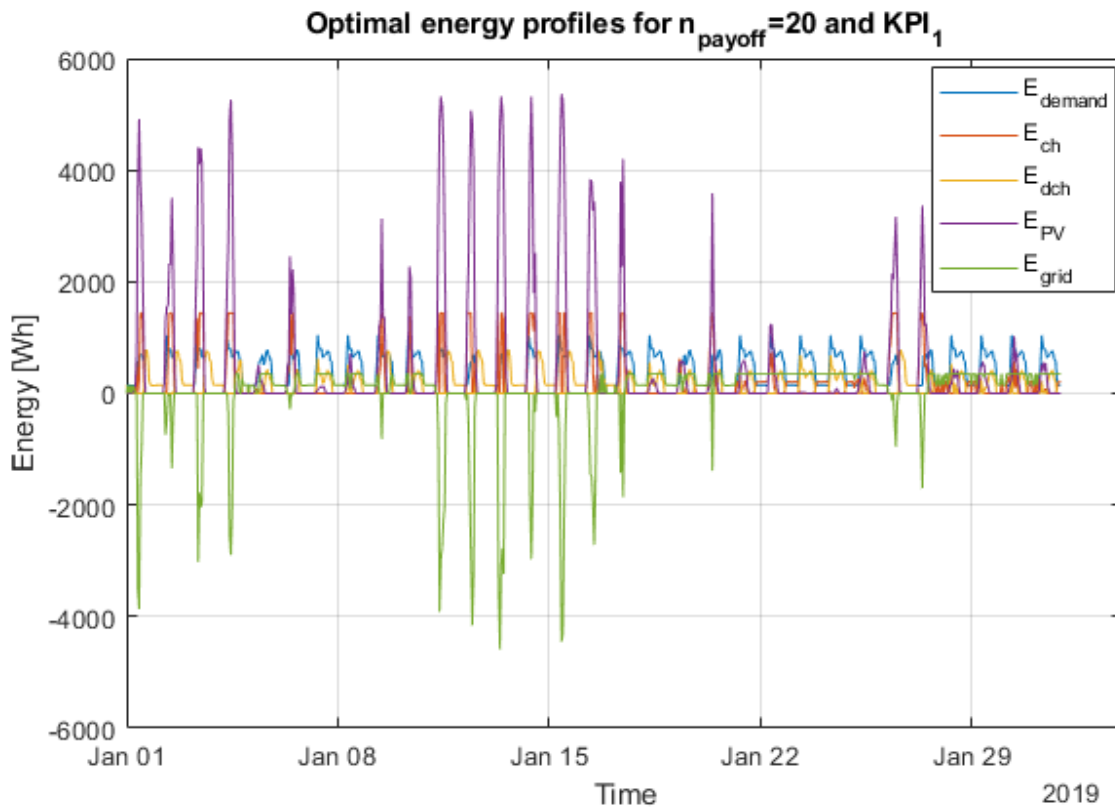
Figure 23. A detail (January) from optimal energy profiles obtained for $n_{payoff} = 20$ and cost function 1 (KPI₁). Values on the y-axis represent energy flows during 1 h intervals.
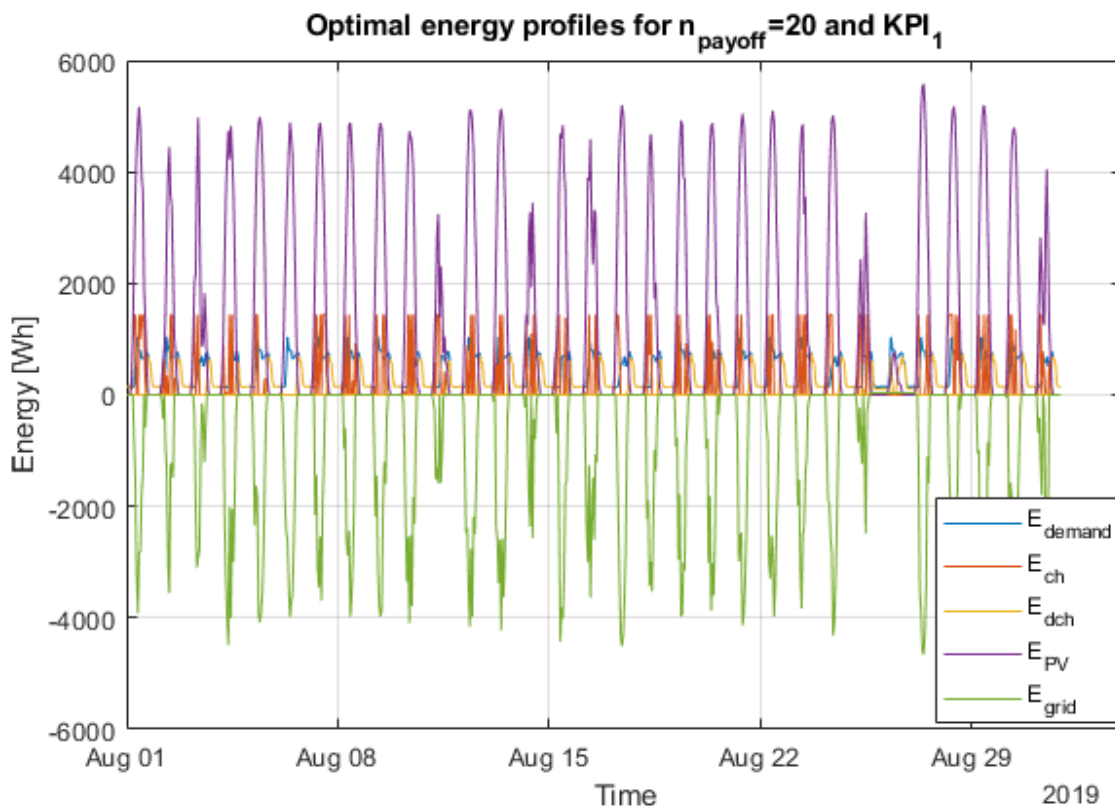
Figure 24. A detail (August) from optimal energy profiles obtained for $n_{payoff} = 20$ and cost function 1 (KPI₁). Values on the y-axis represent energy flows during 1 h intervals.
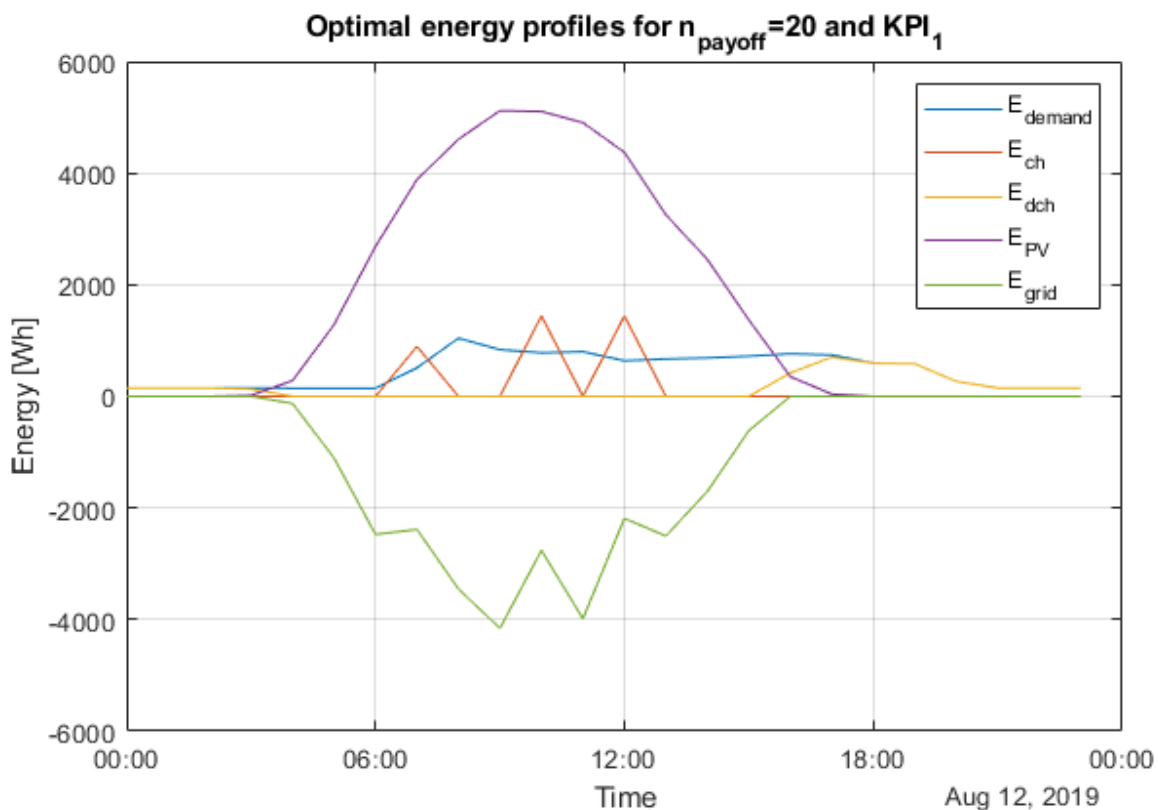
Figure 25. A detail (August 12th) from optimal energy profiles obtained for n_{payoff} = 20 and cost function 1 (KPI$_1$). Values on the y-axis represent energy flows during 1 h intervals.

3.3. Slovenian pilot site in Lendava

EMS tool for the library in Lendava is tailored to compute the optimal daily operation plan of the paraffin based storage system, with respect to varying available temperatures from the geothermal distribution grid, heat dissipation in the storage, and the heat demands from different heating circuits, including minimum required starting temperature to ensure heat supply for the required comfort conditions. Also the usage of existing oil-based heating system is considered as a back-up.

The following functionalities of the Store4HUC EMS are envisioned on the Lendava site.

Off-line:

1) planning the optimal operation of the heat storage by taking into account typical daily heat demands of the existing HUC setup for different pre-determined return on investment periods, with respected HUC-induced constraints;

Thus module (2) is applied on the Lendava site.

3.3.1. Module (2) results for the Lendava pilot site

The paraffin-based storage model needs to include the effect of phase change of paraffin on temperatures which are typical for exploitation which enlarges its effective heat capacity. It includes two typical areas of operation, with two sub-areas in each:

1. Effective temperature in the storage is less or equal than the melting temperature of the paraffin –
   - the storage heating or cooling is performed based on the difference between the heat taken from the sources and the heat demand, in the following way:

a. If the mass of liquid paraffin is higher than zero, it is decreased (mass of solid paraffin increased) to release net heat needed or increased (mass of solid paraffin decreased) to absorb the net heat provided

b. If the mass of liquid paraffin is zero, the temperature of the solid paraffin mass is decreased to provide the net heat needed and increased to absorb the net het provided

2. Effective temperature in the storage is greater than the melting temperature of the paraffin –- the storage heating or cooling is performed based on the difference between the heat taken from the sources and the heat demand, in the following way:

a. If the mass of solid paraffin is higher than zero, it is decreased (mass of liquid paraffin increased) to absorb the net heat provided or increased (mass of liquid paraffin decreased) to provide the net heat needed

b. If the mass of solid paraffin is zero, the temperature of the liquid paraffin mass is increased to absorb the net heat provided or decreased to provide the net heat needed

The control inputs are the thermal energy taken from the geothermal heat distribution grid and the heat taken from the oil-based boiler as the safe alternative. The disturbance input is the thermal energy needed to heat the library.

The optimization criterion is a combination of KPI2 (external energy cost), KPI3 (Average CO2 emission) and KPI5 (Use of energy for RES). The daily profiles of control inputs are optimized for the given thermal demand and geothermal heat distribution network constraints, by employing a SLP to provide optimal daily behaviour of the system of heat sources and paraffin-based storage.

3.4. Austrian pilot site in Weizberg

The pilot site in Weizberg undertakes the installation of a heat energy storage system to enable more efficient operation of the central biomass-based heating station and to be able to supply the buildings of the parish complex with heat while considering the limited capacity of the heat distribution infrastructure.

Task of the EMS tool for the case of Weizberg will be to plan the optimal daily operation of the storage system in different heat demand conditions in the parish complex – it will take into account the heat dissipation in the storage, minimum required starting temperature to ensure heat supply for the required comfort conditions, required temperature conditions in the storage for efficient and long-life operation of the biomass-based boilers.

Based on the computed optimal daily behaviours for different demand conditions it will be possible to program the behaviour of the system accordingly.

The following functionalities of the Store4HUC EMS are envisioned on the Weizberg site.

Off-line:

1) planning the optimal operation of the storage by taking into account daily heat demands of the existing HUC set-up with respected HUC-induced constraints as well as heat biomass-based heat generation costs, if applicable;

Thus module (2) is applied on the Weizberg site.

3.4.1. Module (2) results for the Weizberg pilot site

The Weizberg pilot site already has monitoring and data collection implemented, therefore the real data from January 17th, 2019 was used. The data did not need any interpolation since it did not have any missing

points, but it had been collected with 10 min intervals, so it was resampled to 15 min intervals as module (2) requires. The profile of the power demand is shown in Figure 26, while the profile of the demand flow is shown in Figure 27. The storage tank is placed outside, thus the environment temperature of the storage tank is the outside air temperature. Those measurements are also available and depicted in Figure 28.
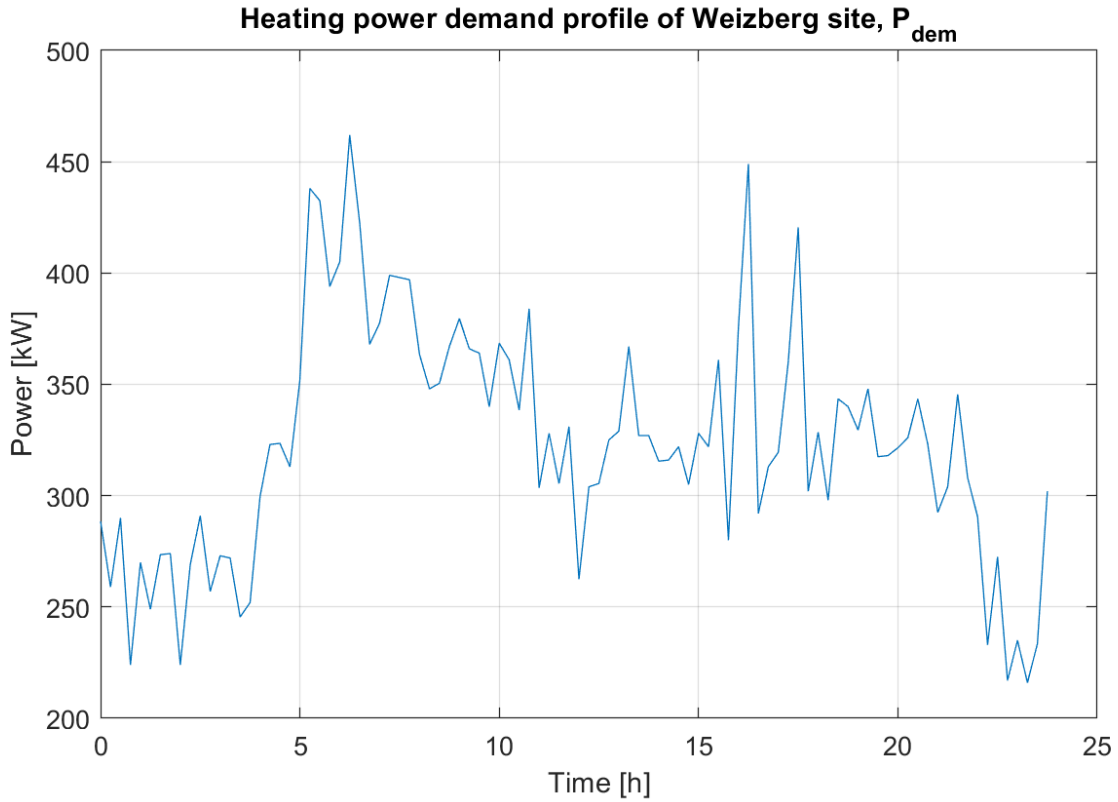
Figure 26. Heating power demand profile of Weizberg site.
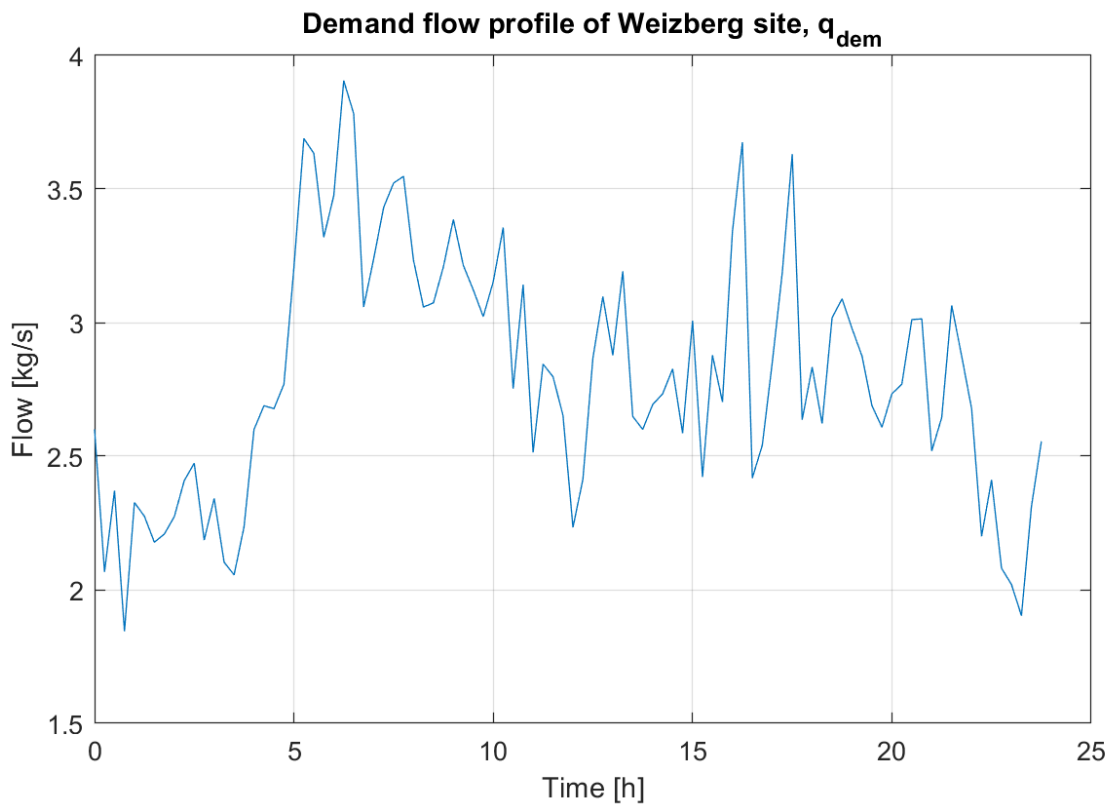
Figure 27. Demand flow profile of Weizberg site.
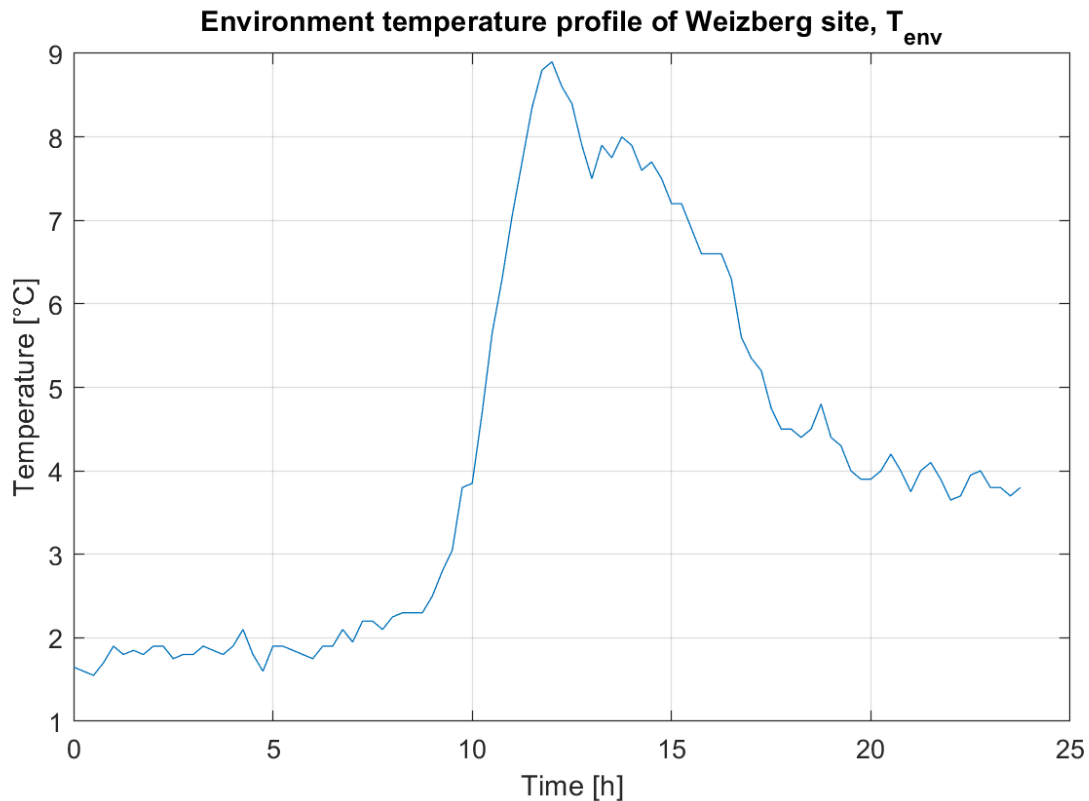
Figure 28. Environment temperature profile of Weizberg site.

The storage tank itself has a cylindrical shape with rounded top and bottom. For simplicity, it is considered with flat top and bottom, so its original height is reduced to match its original volume. Reduced height is denoted with h_{tank}, and the radius with r_{tank}. The heating medium is water. The tank is stratified to 6 equally high layers because temperature sensors will be placed equally spaced along the height of the tank. Layer 1 is the top one and layer 6 is the bottom one. Mass of water in each layer is calculated as $m_l = r_{tank}^2 \pi h_l \rho_w$, where h_l is height of the layer and ρ_w is the density of water. Since all the layers are equally sized it can be written $m_1 = m_2 = m_3 = m_4 = m_5 = m_6 = m$, as well as $h_1 = h_2 = h_3 = h_4 = h_5 = h_6 = h_{layer}$. It has 2 available heat sources, both being woodchip boilers of different rated powers. Later on, $hs1$ and $hs2$ will be indices of variables concerning heat source 1 and heat source 2 respectively. Demand side is a network supplying 12 buildings, but as stated in chapter 2.2, it is simplified to a "black box" where only total power and flow are known. Part of mechanical drawings with included storage tank layers and labels is shown in Figure 29.
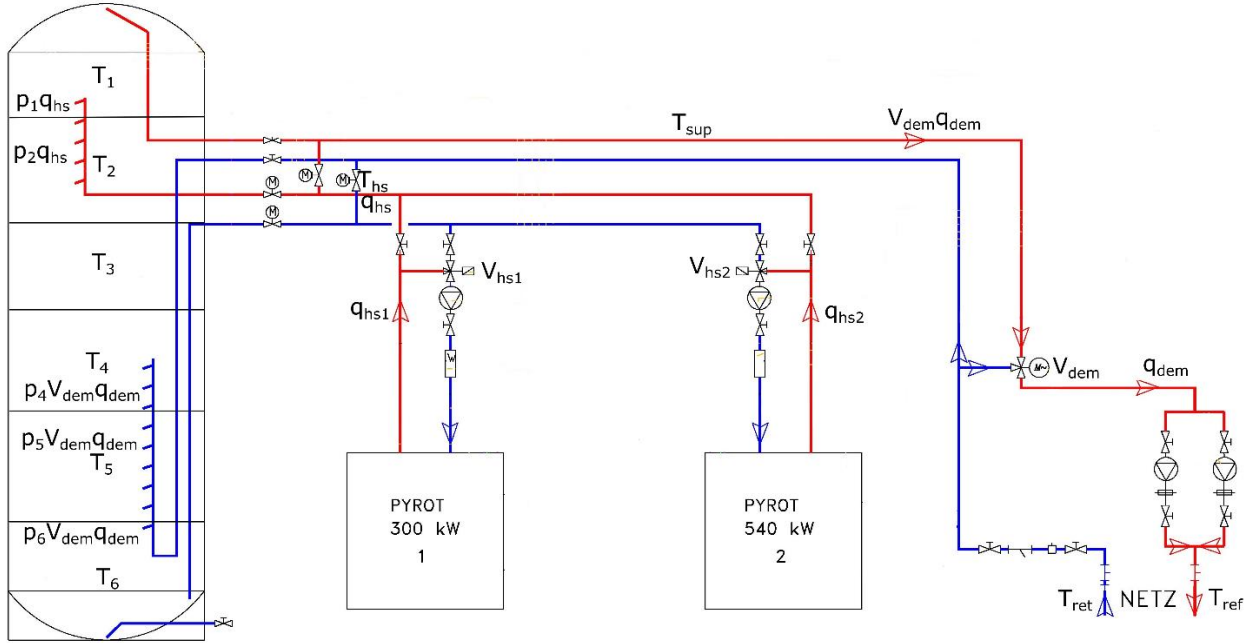
Figure 29. Part of mechanical drawing of the Weizberg pilot site with labels and stratified storage tank.

A noticeable difference between this storage tank and the one from Bračak is how the piping is implemented. Here, inlet pipes go into the tank and disperse input medium at different heights, i.e. input flow is divided between different layers. Input flow coming from the heat sources, q_{hs}, is entering the tank in layer 1 with fraction p_1 and layer 2 with fraction p_2. Input flow coming from the network, $V_{dem}q_{dem}$, is entering the tank in layers 4, 5 and 6 with fractions p_4, p_5 and p_6 respectively.

Another difference is the mixing valve just before the network, V_{dem}. It is used to adjust temperature going to the network if the temperature of layer 1 is higher than the required temperature.

Following Figure 29 and expressions (2.2.3) – (2.2.6) from chapter 2.2.1, non-linear continuous-time model of the heat storage tank of the Weizberg pilot site is:

$$mc_p \frac{dT_1}{dt} = q_{21}c_pT_2 - q_{12}c_pT_1 + p_1q_{hs}c_pT_6 + p_1P_{hs1} + p_1P_{hs2} - V_{dem}q_{dem}c_pT_1$$
$$- (k_c + k_{b12})\frac{A_h}{\Delta x}(T_1 - T_2) - hA_{w1}(T_1 - T_{env}),$$
(3.4.1)

$$mc_p \frac{dT_2}{dt} = q_{12}c_pT_1 - q_{21}c_pT_2 + q_{32}c_pT_3 - q_{23}c_pT_2 + p_2q_{hs}c_pT_6 + p_2P_{hs1} + p_2P_{hs2}$$
$$+ (k_c + k_{b12})\frac{A_h}{\Delta x}(T_1 - T_2) - (k_c + k_{b23})\frac{A_h}{\Delta x}(T_2 - T_3)$$
$$- hA_{w2}(T_2 - T_{env}),$$
(3.4.2)

$$mc_p \frac{dT_3}{dt} = q_{23}c_pT_2 - q_{32}c_pT_3 + q_{43}c_pT_4 - q_{34}c_pT_3 + (k_c + k_{b23})\frac{A_h}{\Delta x}(T_2 - T_3)$$
$$- (k_c + k_{b34})\frac{A_h}{\Delta x}(T_3 - T_4) - hA_{w3}(T_3 - T_{env}),$$
(3.4.3)

$$mc_p \frac{dT_4}{dt} = q_{34}c_p T_3 - q_{43}c_p T_4 + q_{54}c_p T_5 - q_{45}c_p T_4$$

$$+ p_4 V_{dem} q_{dem} c_p \left(T_1 - \frac{P_{dem}}{V_{dem} q_{dem} c_p}\right) + (k_c + k_{b34})\frac{A_h}{\Delta x}(T_3 - T_4) \quad (3.4.4)$$

$$- (k_c + k_{b45})\frac{A_h}{\Delta x}(T_4 - T_5) - hA_{w4}(T_4 - T_{env}),$$

$$mc_p \frac{dT_5}{dt} = q_{45}c_p T_4 - q_{54}c_p T_5 + q_{65}c_p T_6 - q_{56}c_p T_5$$

$$+ p_5 V_{dem} q_{dem} c_p \left(T_1 - \frac{P_{dem}}{V_{dem} q_{dem} c_p}\right) + (k_c + k_{b45})\frac{A_h}{\Delta x}(T_4 - T_5) \quad (3.4.5)$$

$$- (k_c + k_{b56})\frac{A_h}{\Delta x}(T_5 - T_6) - hA_{w5}(T_5 - T_{env}),$$

$$mc_p \frac{dT_6}{dt} = q_{56}c_p T_5 - q_{65}c_p T_6 + p_6 V_{dem} q_{dem} c_p \left(T_1 - \frac{P_{dem}}{V_{dem} q_{dem} c_p}\right) - q_{hs}c_p T_6, \quad (3.4.6)$$

where

$$q_{hs} = V_{hs1} q_{hs1} + V_{hs2} q_{hs2}. \quad (3.4.7)$$

Furthermore, mass flows between layers are defined as:

$$q_{12} = \max(0, p_1 q_{hs} - V_{dem} q_{dem}), \quad (3.4.8)$$

$$q_{23} = \max(0, q_{hs} - V_{dem} q_{dem}), \quad (3.4.9)$$

$$q_{34} = \max(0, q_{hs} - V_{dem} q_{dem}), \quad (3.4.10)$$

$$q_{45} = \max(0, q_{hs} - (p_5 + p_6)V_{dem} q_{dem}), \quad (3.4.11)$$

$$q_{56} = \max(0, q_{hs} - p_6 V_{dem} q_{dem}), \quad (3.4.12)$$

$$q_{65} = \max(0, p_6 V_{dem} q_{dem} - q_{hs}), \quad (3.4.13)$$

$$q_{54} = \max(0, (p_5 + p_6)V_{dem} q_{dem} - q_{hs}), \quad (3.4.14)$$

$$q_{43} = \max(0, V_{dem} q_{dem} - q_{hs}), \quad (3.4.15)$$

$$q_{32} = \max(0, V_{dem} q_{dem} - q_{hs}), \quad (3.4.16)$$

$$q_{21} = \max(0, V_{dem} q_{dem} - p_1 q_{hs}). \quad (3.4.17)$$

Coefficient for buoyant conductivity k_b is calculated in each timestamp as defined in expression (2.2.4) and then used as a constant.

Constraints posed by the boilers are responsible for different dynamics of the system in different areas, i.e. they change expressions for bypass valves V_{hs1} and V_{hs2}. Areas of operation are defined by their minimal input temperature, $T_{hs1,in,min} = T_{hs2,in,min} = T_{hs,in,min}$. Maximal input temperature for the boilers is higher than maximal temperature allowed in the storage tank, so it does not set additional constraints.

Constraints to ensure that the system stays in the current area of operation, i.e. to ensure same system dynamics are:

$$T_6(k) + \Delta T_6(k) < T_{hs,in,min}, when\ T_6(k) < T_{hs,in,min} \quad (3.4.18)$$

$$T_{hs,in,min} \leq T_6(k) + \Delta T_6(k), when\ T_{hs,in,min} \leq T_6(k) \quad (3.4.19)$$

Dynamics of bypass valves based on areas of operation:

$$V_{hs1} = \begin{cases} 1, when\ T_6 \geq T_{hs,in,min} \\ \dfrac{P_{hs1}}{P_{hs1} + q_{hs1}c_p(T_{hs,in,min} - T_6)}, when\ T_6 < T_{hs,in,min} \end{cases} \quad (3.4.20)$$

$$V_{hs2} = \begin{cases} 1, when\ T_6 \geq T_{hs,in,min} \\ \dfrac{P_{hs2}}{P_{hs2} + q_{hs2}c_p(T_{hs,in,min} - T_6)}, when\ T_6 < T_{hs,in,min} \end{cases} \qquad (3.4.21)$$

Mixing valve of the heating network V_{dem} operates so that the temperature of the medium going into the network is at certain value:

$$V_{dem} = \begin{cases} 1, when\ T_1 \leq T_{ref} \\ \dfrac{P_{dem}}{P_{dem} + q_{dem}c_p(T_1 - T_{ref})}, when\ T_1 > T_{ref} \end{cases} \qquad (3.4.22)$$

Therefore, at any time instance temperature of layer 1 must be greater than or equal to the required supply temperature, i.e. $T_1 \geq T_{ref}$.

Additional constraint posed by the boilers is the maximal temperature difference between input and output temperature of each of the boilers, $\Delta T_{hs1,max} = \Delta T_{hs2,max} = \Delta T_{hs,max}$. This constraint can be used to determine flows q_{hs1} and q_{hs2}. Boiler pumps can operate with variable flows, but those flows are considered constant for the sake of simplicity, and they are determined as:

$$q_{hs1} = \frac{P_{hs1,max}}{c_p \Delta T_{hs,max}}, \qquad (3.4.23)$$

$$q_{hs2} = \frac{P_{hs2,max}}{c_p \Delta T_{hs,max}}. \qquad (3.4.24)$$

Price for running the boilers, same for both boilers, is calculated through price of woodchips per unit of energy c_{wood} and efficiency of the boilers η_{hs}:

$$c_{hs} = \eta_{hs} c_{wood} T_s. \qquad (3.4.25)$$

Values of constants, parameters, sizes, and prices are:

- constants:
  - density of water, $\rho_w = 986.7 \text{ kg/m}^3$,
  - specific heat capacity of water, $c_p = 4185.1 \text{ J/(kg K)}$,
  - thermal expansion coefficient of water, $\alpha_p = 0.516 \cdot 10^{-3} \text{ K}^{-1}$,
  - von Karman constant, $\kappa = 0.41$,
  - water conductivity coefficient, $k_c = 0.637095 \text{ W/(m K)}$,
  - heat transfer coefficient, $h = 0.085 \text{ W/(m}^2 \text{ K)}$,
- storage tank dimensions:
  - radius of the tank, $r_{tank} = 1.4 \text{ m}$,
  - total height of the tank, $h_{tank} = 6.25 \text{ m}$,
  - height of each layer, $h_{layer} = 1.0417 \text{ m}$,
  - length between midpoints of 2 neighbouring layers, $\Delta x = 1.0417 \text{ m}$,
  - thickness of the insulation, $d_i = 0.3 \text{ m}$
  - fraction of q_{hs} entering layer 1, $p_1 = 0.2$,
  - fraction of q_{hs} entering layer 2, $p_2 = 0.8$,
  - fraction of $V_{dem}q_{dem}$ entering layer 4, $p_4 = 0.3333$,
  - fraction of $V_{dem}q_{dem}$ entering layer 5, $p_4 = 0.5556$,

- o fraction of $V_{dem}q_{dem}$ entering layer 6, $p_4 = 0.1111$;
- operating parameters:
  - o supply temperature, $T_{ref} = 85\,°C$
  - o minimal temperature in layer 1, $T_{1,min} = 85\,°C$,
  - o maximal temperature in layer 1, $T_{1,max} = 95\,°C$,
  - o maximal temperature of water in the tank, $T_{max} = 95\,°C$,
  - o minimal input temperature in boilers, $T_{hs,in,min} = 65\,°C$,
  - o maximal thermal power of boiler 1, $P_{hs1,max} = 300\,kW$,
  - o maximal thermal power of boiler 2, $P_{hs2,max} = 540\,kW$,
  - o mass flow of the boiler 1, $q_{hs1} = 4.7789\,kg/s$,
  - o mass flow of the boiler 2, $q_{hs2} = 8.6019\,kg/s$;
- optimization procedure parameters:
  - o maximal shift in power for boiler 1, $\Delta P_{hs1,max} = 500\,W$,
  - o maximal shift in power for boiler 2, $\Delta P_{hs2,max} = 500\,W$,
  - o convergence tolerance, $conv_{tol} = 0.01€$,
  - o number of non-improved iterations before stopping, $n_{2stop} = 10$,
  - o number of iterations before decreasing maximal shifts in power, $n_{iter,dcrs} = 50$,
  - o coefficient of Δu_{max} decrease, $\lambda_{\Delta u} = 0.8$;
- prices:
  - o price of woodchips, $c_{wood} = 0.03\,€/kWh$,
  - o efficiency of the boilers at nominal power, $\eta_{hs} = 0.85$.

Additional modelling of the Weizberg heating system includes costs of running the boilers at lower powers than their nominal one. With reduced power, boilers are less efficient and require more frequent servicing which in total increases price. Moreover, they emit more pollutant gases while running at reduced power. Therefore, a simulation without this effect modelled would not yield a meaningful result. This effect will be resolved during implementation of the module at the Weizberg pilot site.

4. Conclusions

This deliverable shows the design of the two new modules of the Store4HUC energy management tool. One concerns the optimal parametrization of PV and battery storage system for a site as well as deciding on the optimal operation profile of the battery storage system on the site. The other concerns the computation of the optimal daily operation of heat sources connected to a heat storage tank with known demand, in order to be able to suggest its optimal way of operation.

The modules reside on predictive control and mathematical optimizations, and the underlying mathematical programs are shown for them.

The modules are applied on Store4HUC pilot sites and the obtained results are shown. They give an insight how the historical pilot site can be parametrized (just for the case of PV+battery storage system) and then operated to gain optimal performance in accordance with the set KPIs.

References

[1] Store4HUC deliverable D.T3.1.1. Concept of the adapted existing tools for energy management with energy storages in historical urban centres. September 2019.

[2] 3Smart output T2.1. Modular cross-spanning energy management tool. June 2019. http://www.interreg-danube.eu/3smart

[3] P. Braun, L. Grüne, C. M. Kellett, S. R. Weller & K. Worthmann. Towards price-based predictive control of a small-scale electricity network. International Journal of Control. June 2017.

[4] Store4HUC deliverable D.T2.1.1. Urban key performance indicators. October 2019.

[5] Robert Christopher Buckley. Development of An Energy Storage Tank Model. October 2012.

[6] Casper Amandus Johansen, Bernt Lie, Nils-Olav Skeie. Models for control of thermal energy in buildings. August 2019.

[7] Viessmann Werke GmbH&Co KG. VITOBLOC 200 Tip EM-6/15 technical description.